Progress in Earth and Planetary Science

RESEARCH ARTICLE Open Access

Formation of undulating topography and gravel beds at the bases of incised valleys: Last Glacial Maximum examples beneath the lowlands facing Tokyo Bay

Susumu Tanabe[1*] and Yoshiro Ishihara[2]

Abstract

Recent studies using well density distributed borehole logs have revealed undulating topography at the bases of incised valleys formed during the Last Glacial Maximum (LGM). In this study, from analysis of 4702 borehole logs, undulating topography forming a series of pits 1–2 km long, < 1 km wide, 5–10 m deep, and spaced at 1–2-km intervals was discovered at the bases of LGM incised valleys beneath the Tama River Lowland on the west coast of Tokyo Bay. This undulating topography can be attributed to scouring at braided river channel confluences. In the study area, single borehole logs are available within each 187 m × 187 m grid cell, and the logs sample both the bottom and marginal portions of the scouring, which suggests that this undulating topography is not an artifact of erroneous values arising from mathematical interpolation. The morphologies and incision depths of two incised valleys in the study area show a cover effect of the gravel bed at the base of the post-LGM incised-valley fills. The basal age of this basal gravel bed (BG) is confirmed at < 30 ka because the LGM incised valleys dissect the MIS 3 Tachikawa buried terrace overlain by the AT tephra dated 30.0 ka. This means that the BG, which represents braided-river sediments, is interpreted as resulting from the LGM sea-level lowstand after 30 ka.

Keywords: Basal gravel bed (BG), Braided river, Scour, Cover effect, Sea-level change, AT tephra

1 Introduction

An incised valley is a topographic feature formed by river incision related to allogenic forcing such as sea-level lowering (Dalrymple et al. 1994, 2006). Incised valleys were formed in the Last Glacial Maximum (LGM) in many places in the world because of the global lowering of sea level. LGM incised valleys are filled by riverine sediments deposited in association with the subsequent deglacial sea-level rise and stillstand; these sediments, which can comprise fluvial, estuarine, and deltaic sediments from the bottom to the top of the sequence, are termed post-LGM incised-valley fills (e.g., Zaitlin et al. 1994; Tanabe et al. 2015). Modern riverine coastal plains are situated on these post-LGM incised-valley fills. In these kinds of settings, the post-LGM incised-valley fills in riverine coastal plains form the present-day ground surface. The post-LGM incised-valley fills have a high-water content and form unconsolidated soft strata, contributing to various geological hazards such as subsidence caused by groundwater pumping and amplification of earthquake ground motion (e.g., Kaizuka and Matsuda 1982; Endo et al. 2001). The LGM incised valleys constitute a physical boundary between the basement and the post-LGM incised-valley fills. Therefore, the study of the morphology of LGM incised valleys and of the depositional architecture of the post-LGM incised-valley fills are important for mitigation of geological hazards as well

* Correspondence: s.tanabe@aist.go.jp
[1]Geological Survey of Japan, AIST, Central 7, Higashi 1-1-1, Tsukuba 305-8567, Japan
Full list of author information is available at the end of the article

as for unraveling spatial and temporal patterns of coastal landscape development and its controlling factors.

The morphology of incised valleys has been drawn as smooth depth or isopach contours in modern and geological analogues on the basis of human interpretation (e.g., Dalrymple et al. 1994, 2006; Anderson and Rodriguez 2008; Milli et al. 2016; Walsh et al. 2016). However, recently, several studies from Japan have suggested that undulating topography prevails at the bases of LGM incised valleys on the basis of several thousand well density distributed borehole logs obtained for geotechnical purposes. Undulating topography has been reported from the Kanto Plain, including the Tokyo Lowland, central Japan (Tanabe et al. 2008, 2014; Ishihara et al. 2012; Ishihara and Sugai 2017; Tanabe and Ishihara 2020); the Nobi Plain, central Japan (Yamaguchi et al. 2006; Hasada and Hori 2016); and the Osaka Plain, western Japan (Mitamura and Hashimoto 2004; Ito et al. 2018). The undulating topography detected by these studies consists of a series of scours that are 1–10 km long and wide and 3–10 m deep, and are spaced at 1–10-km intervals. Most of these studies reconstructed valley topography on the basis of the mathematically interpolation of the depth values of the valley's bases, and the undulating topography is clearly illustrated in their figures. These undulating topographies might reflect abnormal values calculated by mathematical interpolation; however, they could also be attributed to acceptance of values erroneously interpreted to be false. Similar undulating topography has been reported from the Charente, Lay-Sèvre, and Seude incised valleys on the Atlantic continental shelf off France on the basis of high-density seismic surveys (Chaumillon and Weber 2006; Chaumillon et al. 2008) and even from significantly older geological records of the Lower Cretaceous McMurray Formation in western Canada (Horner et al. 2019) and the upper Pliocene Santa Barbara coalfield in central Italy (Ielpi and Ghinassi 2014) on the basis of abundant well logs.

Tanabe et al. (2008) reconstructed several buried terraces formed after Marine Isotope Stage (MIS) 5e and a 70-m-deep LGM incised valley in a 700 km^2 wide area in the Tokyo Lowland on the basis of correlation among 7000 borehole logs. They discovered undulating topography consisting of a series of scours, each 1 km long and wide and 5 m deep, which occur at 1-km intervals in the incised valley. Tanabe et al. (2014) preliminarily interpreted this topography as representing pools and riffles in the braided river system. However, those studies regarded the top of the basal gravel bed (BG) of the post-LGM incised-valley fill as the base of the incised valley because few borehole logs entirely penetrate the BG, which constitutes a firm ground for the foundations of buildings. The BG in the Tokyo Lowland has a uniform thickness of 5 m; thus, the undulating topography of its top surface is assumed to occur also at the base. Furthermore, there was an area of sparse data in the northern Tokyo Lowland, so some of the undulating topography might reflect abnormal values calculated by mathematical interpolation.

Since 2014, the Geological Survey of Japan (GSJ) has carried out surveys of the Tama River Lowland on the west coast of Tokyo Bay to mitigate geological hazards such as amplification of earthquake ground motion. The Tama River Lowland is a small delta with an area of 120 km^2. The area contains the Tokyo Metropolitan area; therefore, a high-density distribution of borehole logs is available. In the Tama River Lowland, one borehole log is available for each 187 m × 187 m grid cell, and the data density is higher than that of the Tokyo Lowland (316 m × 316 m grid cell). In the Tama River Lowland, consolidated Quaternary strata underlie the post-LGM incised-valley fills, so many borehole logs penetrate the BG.

In this study, we reveal detailed topography of the late Pleistocene buried terraces and of the LGM incised valley on the basis of more than 4700 borehole logs, 12 radiocarbon-dated sediment cores, and six geological cross sections. As a result, the presence of undulating topography at the base of the LGM incised valley, which is not a result of mathematical interpolation, is confirmed, and the basal age of the BG is clarified. Furthermore, we discuss the formation of buried terraces and the LGM incised valleys on the basis of comparison with sea-level changes in and around the LGM. And then, finally, we examine the incision processes of the undulating topography by comparing the modern analogues of scouring at river beds.

2 Regional setting

Tokyo Bay, which has an area of 922 km^2, has a maximum water depth of 70 m but a mean water depth of only 17 m (Fig. 1a, b). The mean wave height in the bay is 0.3 m and the tidal range is 1.8 m. According to the classification scheme of Davis and Hayes (1984), the bay is a tide-dominated coastal environment. Before the seventeenth century, the Tone River, which has the largest catchment in Japan, flowed into Tokyo Bay (Fig. 1b). The course of Tone River was diverted to the Pacific to prevent flooding in the Tokyo urban area (Okuma 1981). The present Tone River drains an area of 16,840 km^2 and has a water discharge of 8.7 km^3/year (276 m^3/s) and a sediment discharge of 3 Mt/year (95 kg/s; Milliman and Farnsworth 2011). At present, the largest river flowing into Tokyo Bay is the Tama River, which drains an area of 1240 km^2 and has a water discharge of 40 m^3/s (Fig. 1c). The Tsurumi River, which was the major tributary of the Tama River during the LGM (e.g., Matsushima 1987), drains an area of 235 km^2 and has a

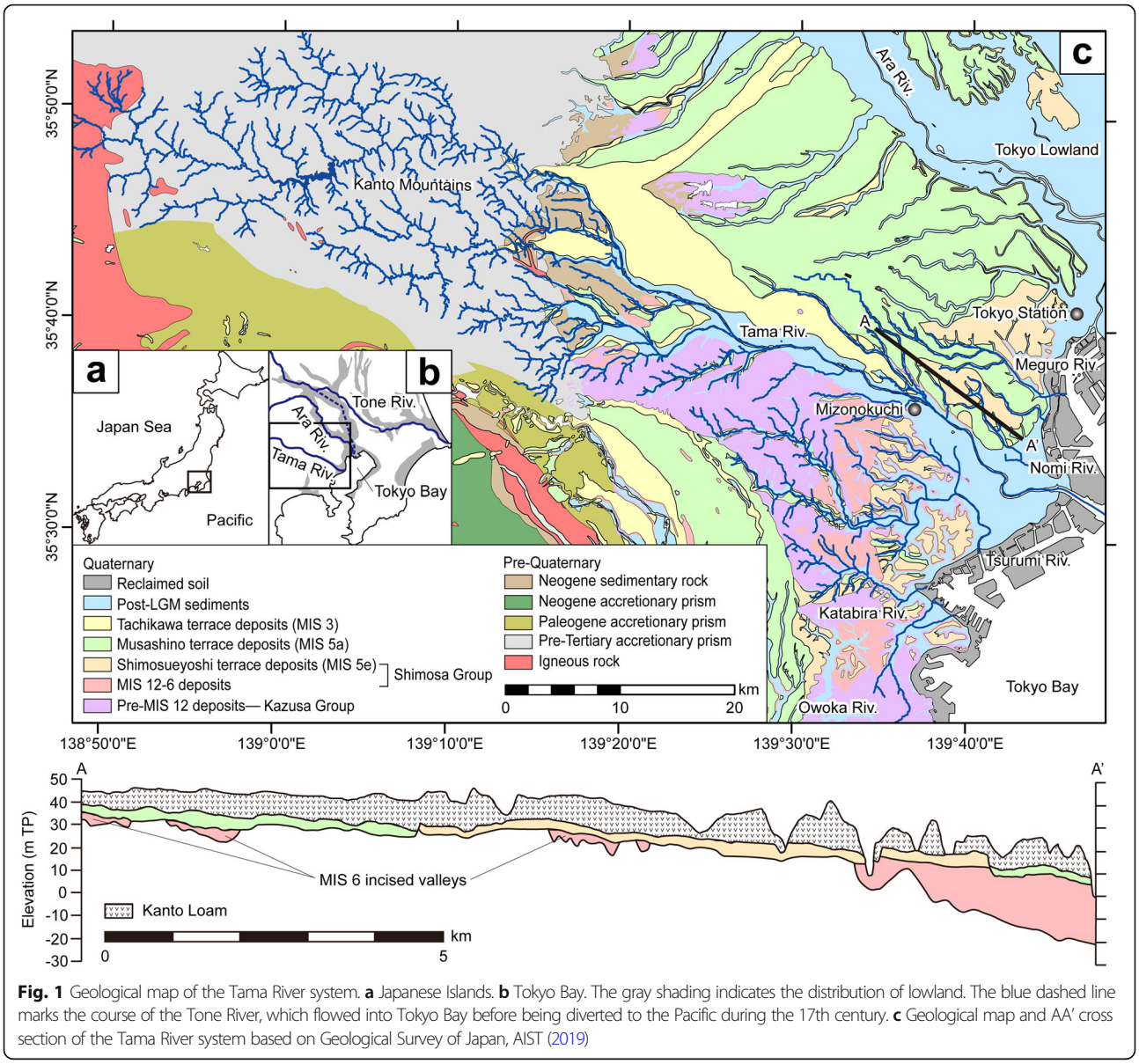

Fig. 1 Geological map of the Tama River system. **a** Japanese Islands. **b** Tokyo Bay. The gray shading indicates the distribution of lowland. The blue dashed line marks the course of the Tone River, which flowed into Tokyo Bay before being diverted to the Pacific during the 17th century. **c** Geological map and AA' cross section of the Tama River system based on Geological Survey of Japan, AIST (2019)

water discharge of 10 m^3/s. The total water discharge of the Tama and Tsurumi rivers is less than one-fifth of that of the Tone River.

The Tama River originates in the Kanto Mountains, 1953 m above the Tokyo Peil datum (TP; mean sea-level at Tokyo Bay), and flows east for 138 km to Tokyo Bay (Fig. 1c). Most of the mountain area consists of a pre-Tertiary accretionary prism, and most of the hills and uplands in the lower reaches of the Tama River are formed of Quaternary sedimentary rocks (Geological Survey of Japan, AIST 2019). The Quaternary strata of the hills and uplands become younger from west to east, and consist of pre-MIS 12 deposits, MIS 12–6 deposits, and MIS 5 deposits (Fig. 1c). The pre-MIS 12 and MIS 12–5 deposits are called the Kazusa and Shimosa groups, respectively.

The MIS 5e deposits of the Shimosa group and the MIS 5a deposits constitute the Shimosueyoshi and Musashino terraces, respectively (Fig. 2). The Shimosueyoshi Terrace is a marine terrace, and occurs on the Shimosueyoshi Upland and part of the Musashino Upland (Fig. 2). The Musashino Terrace is a fluvial strath terrace. The Shimosueyoshi Terrace on the Musashino Upland is a remnant of erosion that provided sediments for the alluvial fans forming the Musashino Terrace (Fig. 1, section AA'). The Shimosa group filling the MIS 6 incised valley forms a relatively soft layer, which extends beneath the Musashino Upland (Fig. 1, section AA', Fig.

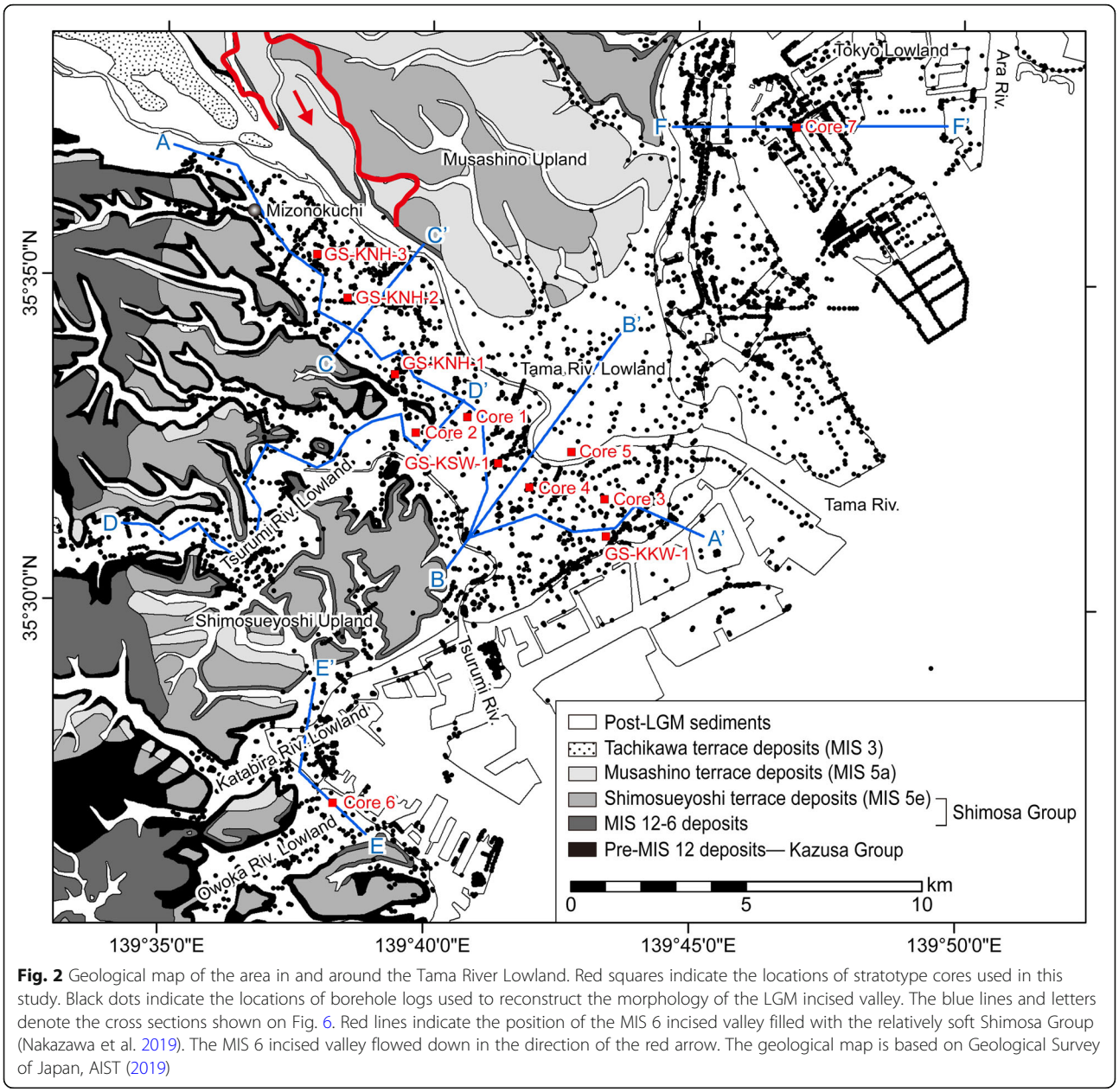

Fig. 2 Geological map of the area in and around the Tama River Lowland. Red squares indicate the locations of stratotype cores used in this study. Black dots indicate the locations of borehole logs used to reconstruct the morphology of the LGM incised valley. The blue lines and letters denote the cross sections shown on Fig. 6. Red lines indicate the position of the MIS 6 incised valley filled with the relatively soft Shimosa Group (Nakazawa et al. 2019). The MIS 6 incised valley flowed down in the direction of the red arrow. The geological map is based on Geological Survey of Japan, AIST (2019)

2; Oka et al. 1984; Nakazawa et al. 2019). The Musashino Terrace is dissected by further lower alluvial fans of the MIS 3 Tachikawa Terrace (Figs. 1c and 2). The Shimosueyoshi, Musashino, and Tachikawa terraces are overlain by aeolian sediments called the Kanto Loam, which is composed mainly of Pleistocene tephra (Fig. 1, section AA'). The Kanto Loam is divided into the Shimosueyoshi, Musashino, and Tachikawa loams, which determine the chronology of the terraces (Fig. 3; Kaizuka et al. 1977). The Shimosueyoshi Terrace has an elevation of 20–40 m TP, and is higher in the southwest (Koike and Machida 2001). The relative sea-level during MIS 5e was 14 m TP in Tokyo Bay (Okuno et al. 2014). From these values, the tectonic uplift rate in this region can be calculated as 0.04–0.21 m/kyr.

The apex of the Tama River Lowland is at 13 m TP at Mizonokuchi (Fig. 2). The gradient of the Tama River becomes gentle at Mizonokuchi, changing from 1.5–4.0/1000 to 0.5–1.0/1000 (Fig. 4). Because of this change, the river style alters from braided to meandering (Kadomura 1961). The lowland is mostly lower than 5 m TP and is composed of floodplain, natural levee, and sand bar sediments. The natural levees and sand bars rise 2 m above the floodplain. The coast of the lowland has been reclaimed since the 1910s. The Tsurumi, Owoka, and Katabira river lowlands are west of the Tama River

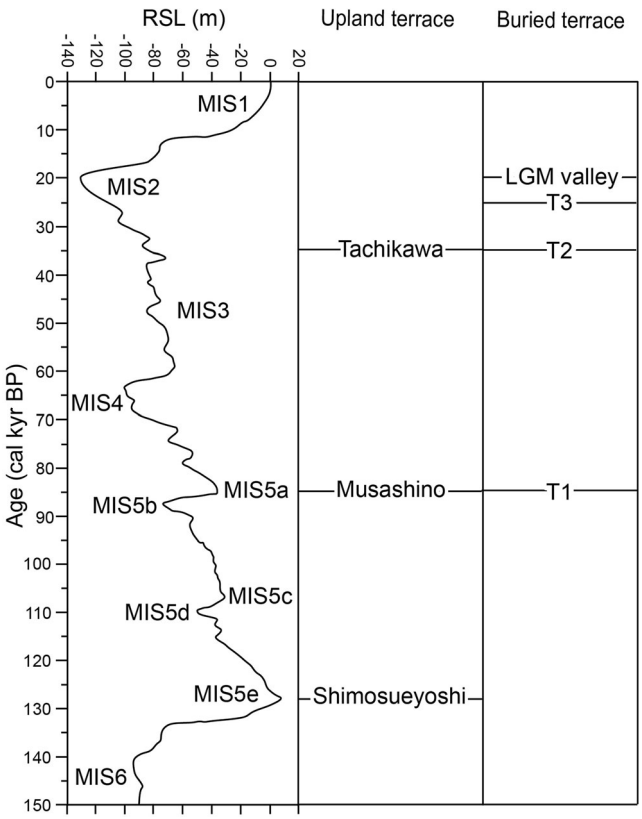

Fig. 3 Correlation of eustatic sea-level changes since MIS 6 and ages of upland terraces around the Tama River Lowland and buried terraces and LGM incised valleys beneath the Tama River Lowland. The sea-level curve is based on Grant et al. (2012). *RSL* relative sea-level, *T1* buried terrace 1, *T2* buried terrace 2, *T3* buried terrace 3, *LGM valley* LGM incised valley

Lowland (Matsuda 1973; Sugimoto and Umehara 1994), while to the east the lowland around the Ara River mouth is called the Tokyo Lowland (Kaizuka et al. 1977; Fig. 2).

The post-LGM incised-valley fills beneath the Tama, Tsurumi, Owoka, and Katabira river lowlands and the Tokyo Lowland unconformably overlie the Kazusa and Shimosa groups (Fig. 5; Matsuda 1973, 1974; Matsushima 1973, 1987; Kaizuka et al. 1977; Oka et al. 1984; Pollution Research Institute, Yokohama City 1988; Sugimoto and Umehara 1994; Port of Tokyo Geological Research Group 2000; Bureau of Port and Harbour, Tokyo Metropolitan Government 2001; Tanabe et al. 2008). The post-LGM incised-valley fills consist of the BG, lower sand bed (LS), lower clay bed (LC), middle sand bed (MS), upper clay bed (UC), upper sand bed (US), and uppermost alluvium bed (UA; Matsuda 1973, 1974; Kaizuka et al. 1977; Oka et al. 1984; Matsushima 1987). The Paleo-Tokyo River Valley, which is filled by

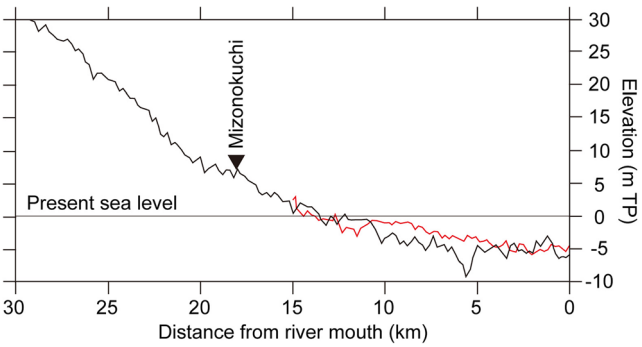

Fig. 4 Thalweg of the Tama (black line) and Tsurumi (red line) river beds. The knickpoint of the Tama River is at Mizonokuchi. The graph is based on Kanto Regional Development Bureau, Ministry of Land, Infrastructure, Transport and Tourism (2017a, b)

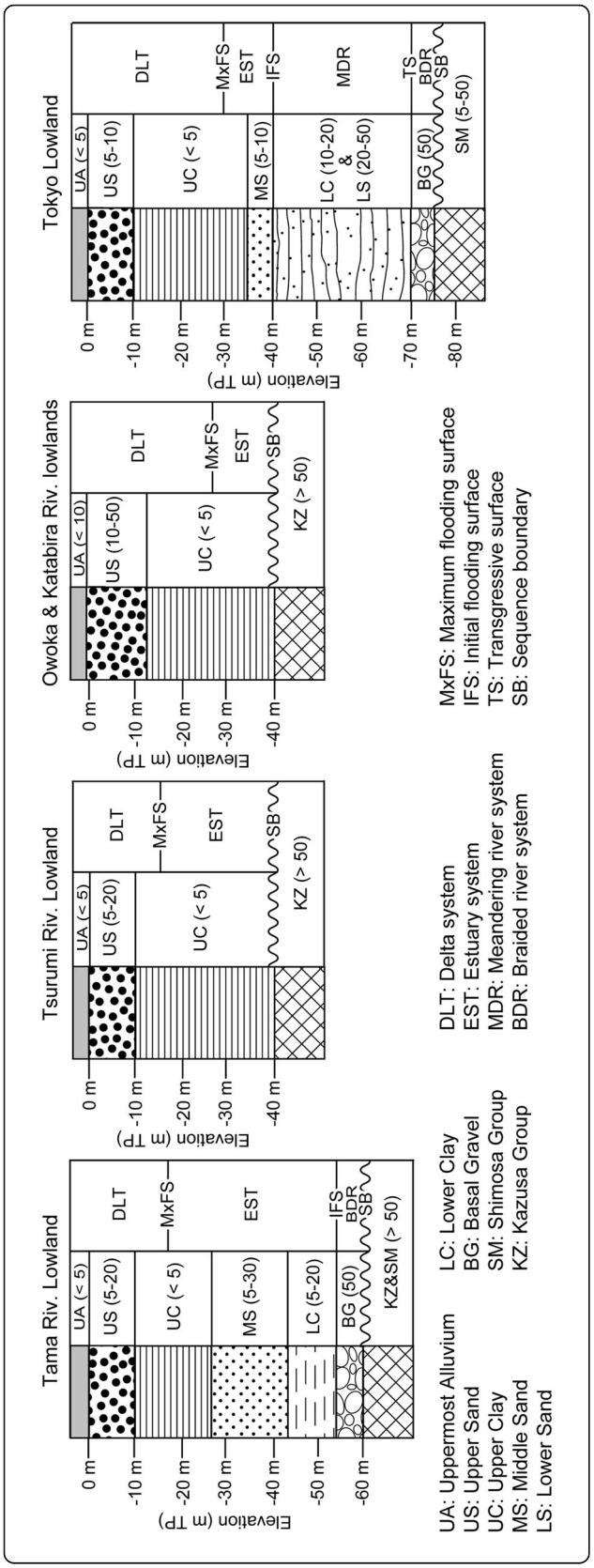

Fig. 5 Correlation of stratotype columns in the Tama, Tsurumi, Owoka, and Katabira river lowlands and the Tokyo Lowland. Lithostratigraphy, sedimentary systems, and bounding surfaces of sequence stratigraphy are correlated as stratotype columns in each lowland

80-m-thick post-LGM sediments beneath the Tokyo Lowland, is the largest LGM valley in the study area, and was formed by the Tone River.

3 Materials and methods

In this study, 8745 borehole logs from Tokyo Metropolis (north of the Tama River) and Kawasaki and Yokohama cities, Kanagawa Prefecture (south of the river) were used (Fig. 2). Of these logs, 3549 were from the Civil Engineering Support and Training Center, Bureau of Construction, Tokyo Metropolitan Government (2019); 2333 were from Kawasaki City (2019); 2330 were from Yokohama City (2019); and 533 were from the Public Works Research Institute (2019).

The borehole logs used for this study were obtained by standard penetration tests for building construction, and all data was prepared as JACIC-formatted XML data (Ministry of Land, Infrastructure, Transport and Tourism 2016). In this format, a borehole log is ruled to contain information on the location (latitude, longitude, and elevation measured by leveling or GPS) and the lithology and *N* value observed/measured every meter. Details of the lithological description differ among borehole drillers; however, lithologies can be roughly classified into gravel, sand, muddy sand, sandy mud, mud, peat, loam, artificial soil, and bedrock. The lithological description also contains information on color and the presence of molluscan shells, burrows, and plant material. The *N* value, which is used in Japan to test ground stiffness, refers to the number of times a 63.5 kg weight must be dropped from a height of 75 cm to penetrate the soil to a depth of 30 cm (Editorial Committee of "Story of *N* value," 1998). *N* values are usually high in coarse sediments and low in fine sediments, and increase with depth because of the effect of compaction. Vertical changes in *N* value are indicative of fining and coarsening trends.

The XML dataset of the borehole logs was converted into a voxel model with 50 m × 50 m × 1 m grid cells by using the interpolation method of Ishihara et al. (2013). Lithology and *N* value cross sections were constructed using this voxel model.

In this study, data from 12 previously reported sediment cores (stratotype cores; Table S1) with 29 radiocarbon dates of plant and shell fragments (Table S2) obtained from the sediment cores were used. Five cores (coded "GS") were recently obtained by the GSJ; these cores yielded detailed facies information including clastic

contents coarser than 4 phi (Fig. S1; Tanabe and Nakashima 2016). However, detailed lithological information was not available for seven cores (cores 1–7 in Table S1; Matsushima, 1987; Matsushima and Yamaguchi, 1987; Port of Tokyo Geological Research Group, 2000); therefore, only the age data were used for these cores. Calibrated ^{14}C ages were calculated with CALIB 7.1 software (Stuiver et al., 2019) using the IntCal13 and Marine13 dataset of Reimer et al. (2013). For calculation of ages from molluscan shells, ΔR (the difference between regional and global marine ^{14}C ages; Stuiver and Braziunas 1993) was regarded as 0 year, and the marine carbon content as 100%. All ages reported here are cal BP (calibrated ^{14}C ages) unless otherwise noted as yr BP (conventional ^{14}C ages).

The stratigraphy of six lithological and *N* value cross sections was interpreted on the basis of correlation with the 12 stratotype cores and previous studies. These cross sections were selected because they represent typical facies succession and architecture of the Tama, Tsurumi, Owoka, Katabira, and Paleo-Tokyo river valley systems in the proximal and distal portions. The base of the post-LGM incised-valley fill was identified on each borehole log by applying the stratigraphic sequence of the six cross sections. Stratigraphic interpretation of the borehole logs was approximately based on Oka et al. (1984) and Matsushima (1987). The Kazusa group consists of sand and mud beds with an *N* value of 50. The *N* values of the mud, sand, and gravel beds of the Shimosa group are 5–20, 20–50, and > 50, respectively, and these sediments are lighter in color than the post-LGM incised-valley fills. The *N* values of the mud, sand, and gravel beds of the post-LGM incised-valley fills are 0–20, 5–30, and 30–50, respectively. The Kazusa and Shimosa groups are lithologically laterally continuous compared to the post-LGM incised-valley fills.

The basal depths of the post-LGM incised-valley fills, the presence of the Kanto Loam on the buried terraces, the presence of a gravel bed in the LGM incised valleys and buried terraces, and the thickness of the gravel bed in each borehole log were extracted manually. The base of the BG was identified as the base of the post-LGM incised-valley fill. The spatial distribution of the LGM incised valley was reconstructed by mathematically interpolating the depth values of the base of the post-LGM incised-valley fill. An interpolation method of ArcGIS 10.6, 3D Analyst tools (Kriging) was applied. It is known that when the density of borehole data points is high enough, the difference in interpolation methods does not affect considerably on the reconstruction of the spatial distribution of the incised valley (e.g., Tanabe et al. 2008; Tanabe and Ishihara 2020). A total of 4702 borehole logs, which penetrate the post-LGM incised-valley fill, were used to reconstruct the spatial distribution of the LGM incised valleys. In 2822 borehole logs, the gravel bed was absent, and the drilling reached to the bedrock of the Kazusa and Shimosa groups. In 1880 borehole logs, the gravel bed was present; those boreholes penetrated the gravel bed and reached the bedrock of the Kazusa and Shimosa groups. The whole study area including the Tama River Lowland has an area of 164 km^2; thus, the density of borehole logs is calculated as one per 187 m × 187 m pixel grid although it is partly inhomogeneous.

4 Results

4.1 Geological cross sections

This section contains a description of the lithologies and *N* values of the Kazusa and Shimosa groups and the post-LGM incised-valley fills in six cross sections extracted from the voxel model (Figs. 2 and 6). We also describe the sedimentary system and the sequence stratigraphic bounding surfaces of the post-LGM incised-valley fills on the basis of the sedimentary facies and radiocarbon dates obtained from the stratotype cores and previous studies (Fig. S1). Based on these data, the depth distributions of the bases of the post-LGM incised-valley fills are described.

4.1.1 Section AA'

Section AA' extends across the Tama River Valley (Fig. 2), which is filled by post-LGM sediments that unconformably overlie the Kazusa and Shimosa groups (Fig. 6; Matsuda 1973; Kaizuka et al. 1977; Oka et al. 1984; Matsushima 1987; Tanabe and Ishihara 2015).

The Kazusa and Shimosa groups consist of sand and mud beds with *N* values > 50. The post-LGM incised-valley fill contains the BG (*N* value = 50), the LC (*N* value = 5–20), the MS (*N* value = 5–30), the UC (*N* value < 5), the US (*N* value = 5–20), and the UA (*N* value < 5), in ascending order (Fig. 5). The BG is correlated to lowstand braided river sediments, the LC, MS, and the lower portion of the UC are correlated to transgressive estuary sediments, and the upper portion of UC, the US, and the UA are correlated to regressive delta sediments (Fig. 5). The braided river sediments mainly consist of clast-supported gravel bed, which is typical in braided river channel environments (Miall 1992). The estuary and delta systems are composed of upward-finning (deepening) and -coarsening (shallowing) sand and mud beds, respectively (Boyd et al. 1992). In the estuary sediments, amount of plant and wood fragments decrease upward, likely recording the river mouth retrogradation, while in the delta sediments, those increase upward, representing the river mouth progradation (Fig. S1; Tanabe and Nakashima 2016). The unconformity between the Kazusa and Shimosa groups and the overlying

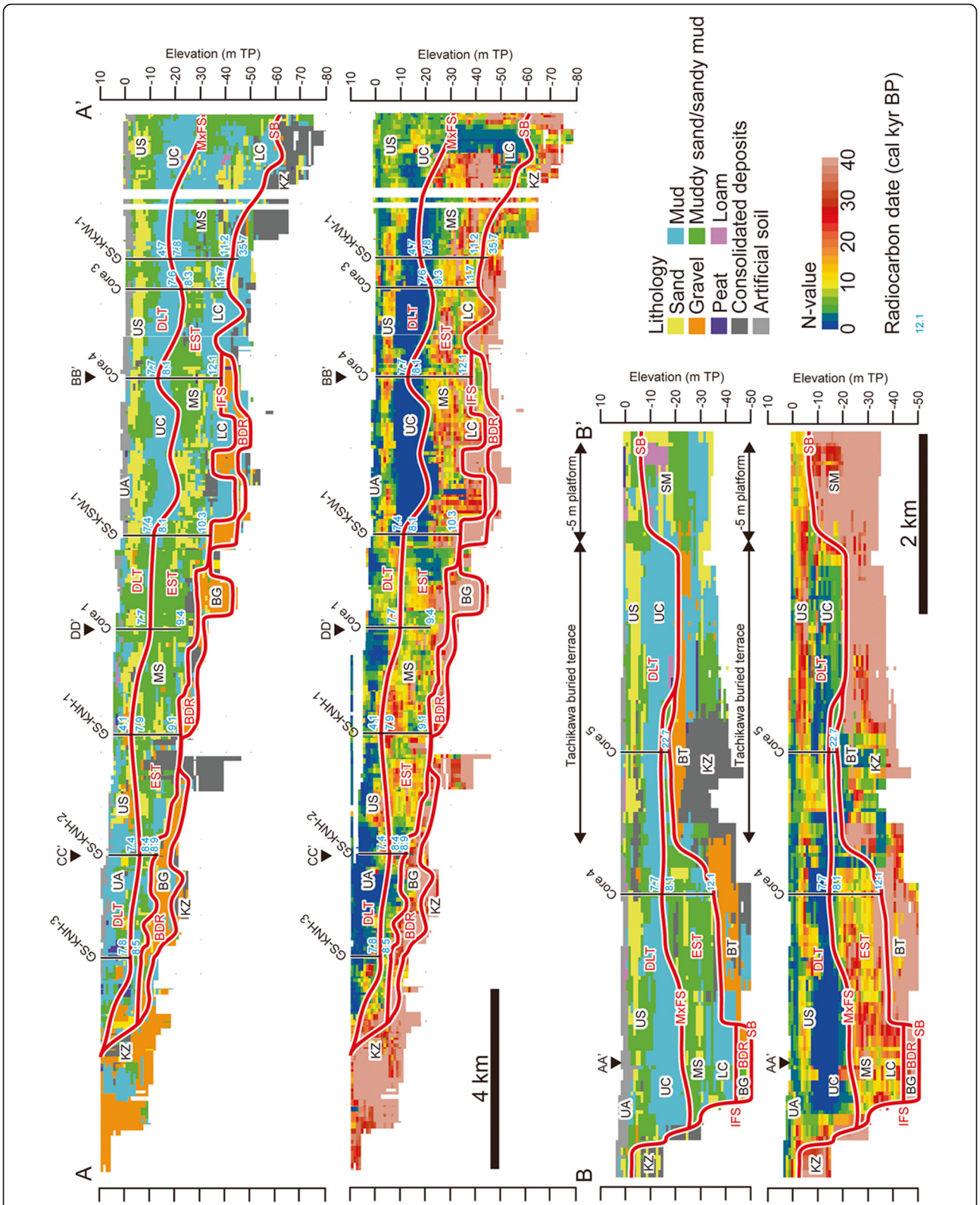

Fig. 6 Cross sections of lithology (upper section in each figure part) and *N* value (lower section in each figure part) in the Tama River Lowland (sections AA', BB', and CC'), the Tsurumi River Lowland (section DD'), the Owoka and Katabira river lowlands (section EE'), and the Tokyo Lowland (section FF'). The traces of cross sections are reported on Fig. 2. Drilling of most borehole logs ceased at the firm surface of the Kazusa and Shimosa groups; therefore, the lithology and *N* value of the pre-LGM deposits are not known for most areas

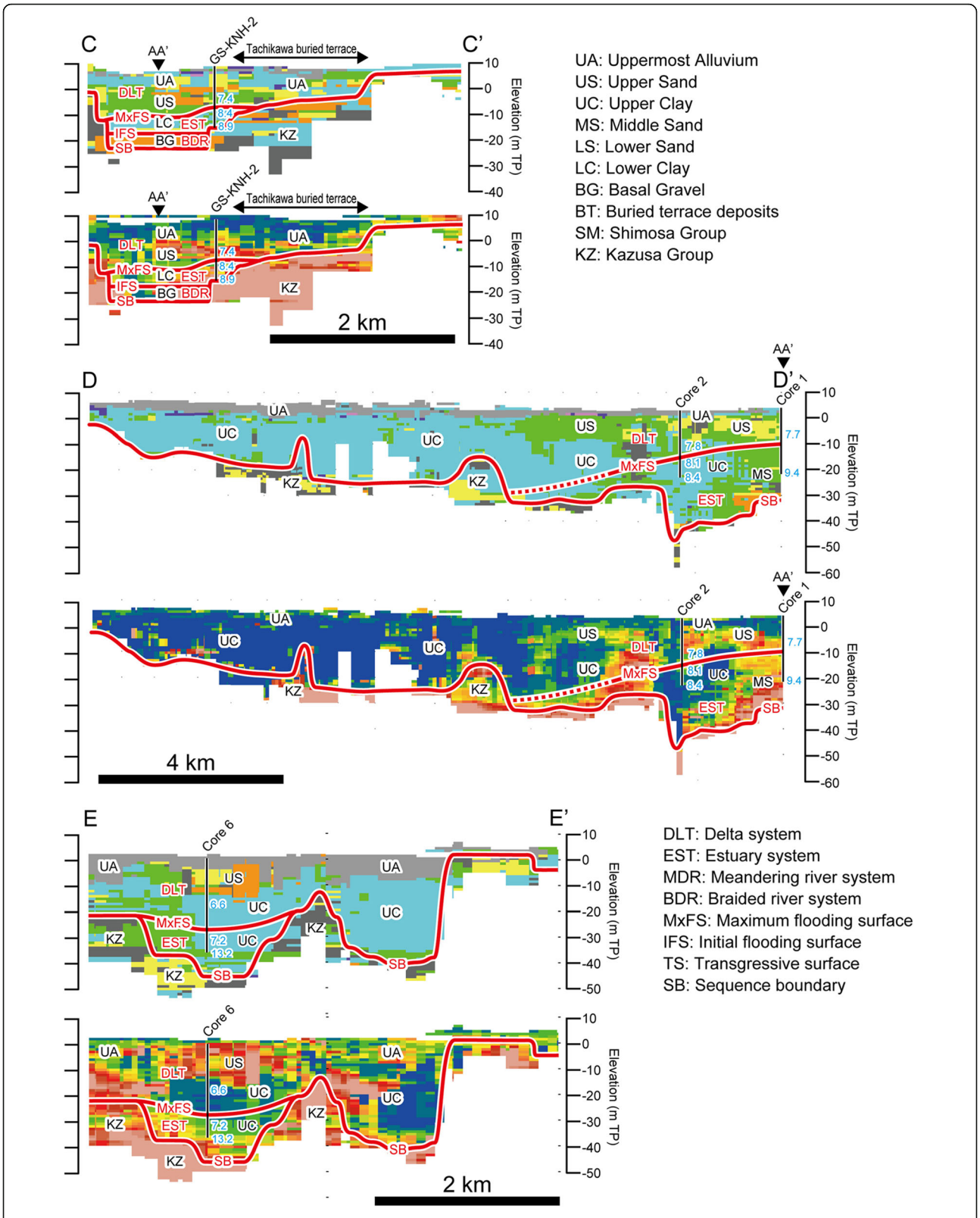

Fig. 6 *(continued.)*

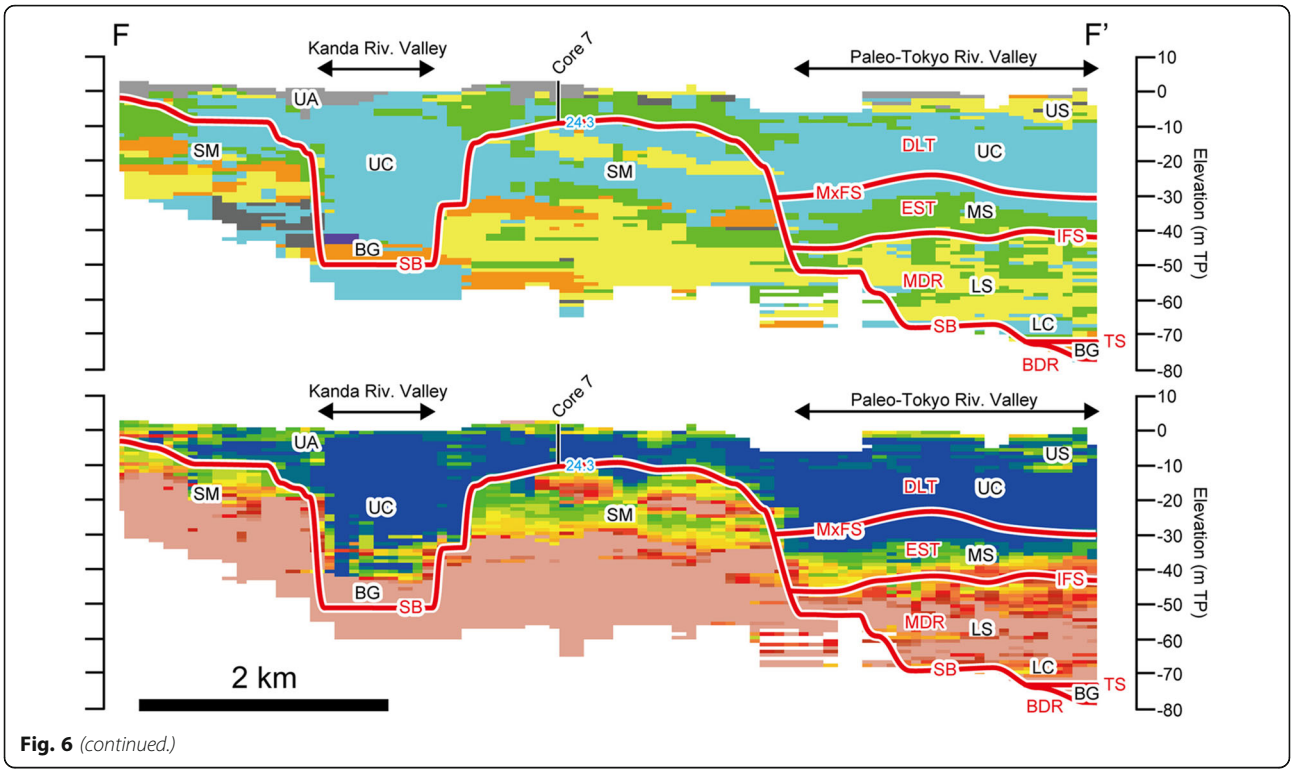

Fig. 6 *(continued.)*

post-LGM incised-valley fills is regarded as a sequence boundary (SB). The boundary between the braided river/estuary sediments represents an initial flooding surface (IFS; a surface of marine flooding onto fluvial sediments; Zaitlin et al. 1994) and the boundary between the estuary/delta sediments represents a maximum flooding surface (MxFS; a surface that separates a retrogradational transgressive system from a progradational highstand system; van Wagoner et al. 1988). Although the LC in the Tokyo Lowland is regarded as part of the transgressive meandering river sediments (Fig. 5; Tanabe et al. 2010), the LC in the Tama River Lowland consists of mud with rootlets and burrows that yield a mixture of marine, brackish, and freshwater diatoms (Fig. S1; Tanabe 2020). Therefore, the LC in the Tama River Lowland is interpreted as salt marsh sediments (Tanabe and Nakashima 2016). These salt marsh sediments are marine sediments, and form part of the estuary sediments.

A radiocarbon date of 35.7 kyr BP shows that the base of the GS-KKW-1 core contains pre-LGM deposits (Figs. S1, 6; Tanabe and Nakashima 2016). Radiocarbon dates from sediments overlying the Kazusa and Shimosa groups and the BG from west of the GS-KKW-1 core range from 12.1 to 8.5 cal kyr BP (ka), and become younger to the west, into the upper reaches of the Tama River Valley (Fig. 6). These dates demonstrate that the estuary sediments onlap the Kazusa and Shimosa groups and the braided river sediments. The MxFS is dated at 7.8 ka in the Tama River Lowland (Fig. 6; Tanabe and Nakashima 2016).

The base of the LGM incised valley can be identified between the Kazusa and Shimosa groups and the braided river sediments or the estuary sediments. The valley has a depth of − 60 m TP in the east and 0 m TP in the west. Undulating topography can be identified at the base of the LGM incised valley (Fig. 6).

4.1.2 Section BB'

Section BB' is a transverse cross section of the Tama River Valley in the southeast of the Tama River Lowland (Fig. 2). In this section, the post-LGM incised-valley fill unconformably overlies the Kazusa group at the valley axis at a depth of − 50 m TP, the Tachikawa buried terrace at − 20 m TP, and the Shimosa group at − 5 m TP (Fig. 6; Matsuda 1973; Oka et al. 1984; Matsushima 1987).

The Kazusa and Shimosa groups (N values > 50) consist of sand and mud beds. The Tachikawa buried terrace contains a gravel bed (N value > 50), and is overlain by the Kanto Loam and peat bed (N values = 5–40), in ascending order. In the valley axis, the post-LGM incised-valley fill consists of the same succession as in

section AA'. The UC, US, and UA overlie the Tachikawa buried terrace, and the US and UA overlie the platform at − 5 m TP (Fig. 6). The UC, US, and UA constitute delta sediments. In Core 4, molluscan shells from − 12.0 and − 11.5 m TP are dated to 8.1 and 7.7 ka, respectively; therefore, the MxFS is at the base of the UC (Fig. 6).

A peat bed at the base of Core 5 is dated to 22.7 ka (Matsushima 1987). This age suggests that the Tachikawa buried terrace had formed before the lowest sea-level of the LGM (20.5 ka; Yokoyama et al. 2018), and may be correlated to MIS 3. The platform at − 5 m TP is regarded as an abrasion platform that formed during the middle Holocene sea-level highstand (Matsuda 1973; Kaizuka et al. 1977). The − 40 m TP platform in this section might have formed between MIS 3 and the LGM (Fig. 6). Details of the − 5 m TP and − 40 m TP platforms are provided in Section 4.2.

4.1.3 Section CC'

Section CC' is a transverse cross section of the Tama River Valley in the northwest of the Tama River Lowland (Fig. 2). In this section, the post-LGM incised-valley fill unconformably overlies the Kazusa group at the valley axis at − 20 m TP and the Tachikawa buried terrace at a platform at − 5 m TP (Fig. 6; Matsuda 1973; Oka et al. 1984).

The Kazusa group and the Tachikawa buried terrace consist of mud and gravel beds (N values > 50), respectively. The post-LGM incised-valley fill consists of the BG, LC, US, and UA at the valley axis, and the UA on the Tachikawa buried terrace (Fig. 6). The LC is correlated to the estuary sediments, and the US and UA are correlated to the delta sediments. In the GS-KNH-2 core, plant fragments from − 6.8 and − 0.2 m TP are dated to 8.4 and 7.4 ka, respectively; therefore, the MxFS is at the base of the US (Figs. S1, 6).

This section is located in the extension of the MIS 6 incised valley (Fig. 2; Nakazawa et al. 2019). However, the MIS 6 incised-valley fill, the Shimosa group that consists of 20-m-thick massive mud (N value < 5; Nakazawa et al. 2019), is not present in this section, which indicates that the MIS 6 incised-valley fill was eroded during formation of the MIS 3 Tachikawa terrace or the LGM incised valley.

4.1.4 Section DD'

Section DD' extends across the Tsurumi River Valley (Fig. 2), which is filled by post-LGM sediments unconformably overlying the Kazusa group (Fig. 6; Matsuda 1973; Oka et al. 1984; Matsushima 1987).

The Kazusa group consists of sand and mud beds (N value > 50). The post-LGM incised-valley fill consists of the UC (N value < 5), the US (N value = 5–20), and the UA (N value < 5), in ascending order. The lower portion of the UC is correlated to the estuary sediments, and the upper portion of the UC, the US, and the UA are correlated to the delta sediments (Fig. 5). To the west, the sand bed of the US changes laterally into a sandy mud/muddy sand bed, and the N value decreases as a result of this lithological change (Fig. 6). A 7.8-ka isochron (MxFS) is located at − 10 m TP in Core 1 and − 15 m TP in Core 2, and dips downward toward the west (Fig. 6). The detection of this surface can be explained as a result of the progradation of a flood-tidal delta to the bay head portion of the Paleo-Tsurumi Bay during the middle Holocene highstand (Matsushima 1987). The unconformity between the Kazusa group and the post-LGM incised-valley fills is regarded as the SB.

In this section, the BG is absent at the base of the post-LGM incised-valley fill, which is at depths of − 40 to 0 m TP, but undulating topography prevails at the base (Fig. 6).

4.1.5 Section EE'

In section EE', the Owoka and Katabira river valleys (Fig. 2) are filled by post-LGM sediments that unconformably overlie the Kazusa group (Fig. 6; Matsushima 1973; Sugimoto and Umehara 1994).

The Kazusa group consists of sand and mud beds (N values > 50). The valley fills consist of Holocene marine mud and sand, which is composed of the UC, US, and UA (Fig. 5). The UC has N values < 5; the US has N values 10–50; and the UA has N values < 10. The lower portion of the UC and the upper portion of the UC, the US, and the UA correspond to estuary and delta sediments, respectively. The unconformity between the Kazusa Group and the post-LGM incised-valley fills are regarded as the SB. The modern Owoka and Katabira rivers have low sediment discharge. Tanabe et al. (2015) reported that the age of the MxFS corresponds with the middle Holocene sea-level highstand of 7 ka in an embayment with low sediment discharge in the Tokyo Lowland. Sugimoto and Umehara (1994) reported radiocarbon dates of 7.2 ka (− 33 m TP) and 6.6 ka (− 18 m TP) in the vicinity of Core 6; therefore, the MxFS must be at ca. − 30 m TP in the Owoka River Lowland (Fig. 6). The US in the Owoka River Lowland is interpreted as spit sediments (Matsushima 1973); this unit is absent in the Katabira River Lowland. The spit sediments are local marine sand bed representing upward-coarsening (shallowing) lithological succession associated with upward increase in reworked shell fragments (Tanabe et al. 2015).

The buried terrace and BG are absent from this cross section. The bases of the LGM incised valleys are above − 45 m TP (Fig. 6).

4.1.6 Section FF'

In section FF' across the Tokyo Lowland (Fig. 2), the post-LGM incised-valley fill unconformably overlies the Shimosa Group (Fig. 6; Matsuda 1974; Kaizuka et al. 1977; Port of Tokyo Geological Research Group 2000; Bureau of Port and Harbour, Tokyo Metropolitan Government 2001).

In the east and west, the Shimosa group is dissected by the Paleo-Tokyo and Kanda river valleys, respectively (Fig. 6). The lower half of the Shimosa group consists of a sand bed (*N* value > 50); the upper half contains a sand bed (*N* value = 20–50) and a mud bed (*N* value = 5–10). The strata of the Shimosa group dip 0.2–0.3° to the east (Fig. 6). The post-LGM Paleo-Tokyo River Valley fill consists of the BG (*N* value = 50), the LS (*N* value = 20–50), the LC (*N* value = 10–20), the MS (*N* value = 5–10), the UC (*N* value < 5), the US (*N* value = 5–10), and the UA (*N* value < 5), in ascending order (Fig. 5; Matsuda 1974; Kaizuka et al. 1977). The BG is correlated to the braided river sediments, the LS and LC are correlated to the meandering river sediments, the MS and the lower portion of the UC are correlated to the estuary sediments, and the upper portion of the UC, the US, and the UA are correlated to the delta sediments. The meandering river sediments consist of alternation of fluvial channel sand and floodplain mud (Tanabe et al. 2015). The SB is at the base of the BG. A transgressive surface (TS; a surface that separates a progradational or aggradational lowstand system from a retrogradational transgressive system; van Wagoner et al. 1988; Catuneanu 2006) is at the braided/meandering river sediments boundary (Fig. 5). The base of the estuary sediments corresponds to the IFS, and the MxFS separates the estuary and delta sediments (Fig. 5; Tanabe et al. 2010). The post-LGM Kanda River Valley fill consists of the BG (*N* value > 50), the UC (*N* value < 5), and the UA (*N* value = 5), in ascending order (Fig. 6).

There is a platform at − 10 m TP between the Paleo-Tokyo and Kanda river valleys (Fig. 6). This platform is regarded as an abrasion platform formed during the middle Holocene sea-level highstand (Matsuda 1974; Kaizuka et al. 1977; Bureau of Port and Harbour, Tokyo Metropolitan Government 2001). However, the basal peat of Core 7 is dated to 24.3 ka, and the Hk-TP tephra (MIS 4; Machida and Arai 2003) has been obtained from the Kanto Loam beneath the basal peat. These ages suggest that this platform can be correlated with the MIS 5a Musashino terrace (Port of Tokyo Geological Research Group 2000) or a certain terrace formed between MIS 5a and MIS 4 (Fig. 3). The Paleo-Tokyo and Kanda river valleys are at levels shallower than − 75 m TP and − 50 m TP, respectively (Fig. 6).

4.2 Distribution of incised valleys and buried terraces

The depth distribution of the bases of the LGM incised valleys and the buried terraces in the Tama, Tsurumi, Owoka, and Katabira river lowlands and the Tokyo Lowland are illustrated in Fig. 7.

The Tama River Valley lies to the south of the present Tama River, and the valley's deepest point is at − 70 m TP in the vicinity of the Tama River mouth. The Tsurumi River Valley merges with the Tama River Valley, and the elevation at the convergence point is − 40 m TP. The deepest points in the Owoka and Katabira, Paleo-Tokyo, and Kanda River valleys are at − 45, − 80, and − 50 m TP, respectively. The Haneda River Valley is a small incised valley (maximum depth − 40 m TP) between the Kanda and Tama river valleys (Fig. 7; Bureau of Port and Harbour, Tokyo Metropolitan Government 2001). The topography of these valleys does not differ very much from that obtained in previous studies (Matsuda 1973, 1974; Kaizuka et al. 1977; Oka et al. 1984; Matsushima 1987; Pollution Research Institute, Yokohama City 1988; Port of Tokyo Geological Research Group 2000; Bureau of Port and Harbour, Tokyo Metropolitan Government 2001; Tanabe et al. 2008); however, the resolution used in this study (187 m × 187 m grid cells) is higher than that of all previous studies.

A platform at − 15 to − 5 m TP lies between the Paleo-Tokyo and Tama river valleys, and a gentle slope at − 20 to 5 m TP and a platform at − 40 m TP lie in the north of the Tama River Valley (Figs. 7 and 8). These platforms are considered as buried terraces. The platform at − 15 to − 5 m TP, the gentle slope at − 20 to 5 m TP, and the platform at − 40 m TP are named buried terrace 1 (T1), buried terrace 2 (T2), and buried terrace 3 (T3), respectively (Fig. 8). The T1 is an abrasion platform formed during the middle Holocene sea-level highstand, superimposed on and reshaping the older MIS 5a–4 terrace, with the latter having on its top the Hk-TP tephra of the Kanto Loam (Fig. 3; Matsuda 1974; Kaizuka et al. 1977; Port of Tokyo Geological Research Group, 2000; Bureau of Port and Harbour, Tokyo Metropolitan Government 2001). The locations at which the Kanto Loam is identified in borehole logs are marked with white dots in Fig. 7. The Kanto Loam is common in the northern part of the T1 between the Paleo-Tokyo and Kanda river valleys, which supports the correlation of the platform with the MIS 5a Musashino Terrace by the Port of Tokyo Geological Research Group (2000). The T2 can be correlated with the MIS 3 Tachikawa Terrace that crops out northwest of Mizonokuchi (Figs. 1c, 2, and 3; Matsuda 1973; Kaizuka et al. 1977; Oka et al. 1984). The gradient of the Tachikawa Terrace is consistent (3/1000–4/1000) from the edge of the buried terrace at − 20 m TP to the apex of the alluvial fan at 180 m TP. The AT tephra, which is dated to 30.0 ka (Smith et al. 2013), is found in the Kanto Loam of the outcrop of the Tachikawa Terrace. Therefore, the gentle slope (i.e., the buried terrace) must have formed before 30.0 ka, and represents the continuation of an alluvial fan

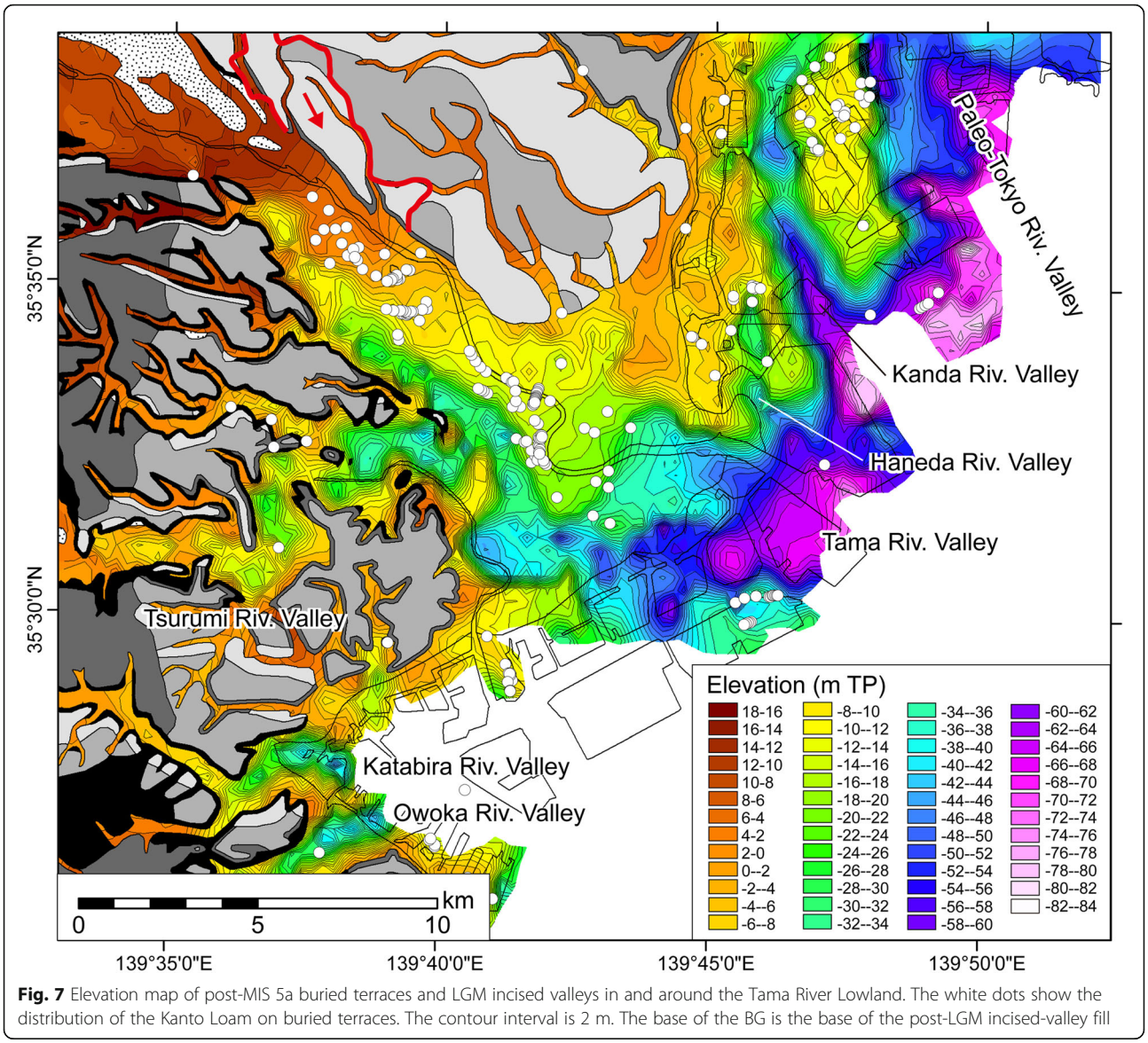

Fig. 7 Elevation map of post-MIS 5a buried terraces and LGM incised valleys in and around the Tama River Lowland. The white dots show the distribution of the Kanto Loam on buried terraces. The contour interval is 2 m. The base of the BG is the base of the post-LGM incised-valley fill

or a braided river from the upper reaches. The Kanto Loam does not overlie the T3 and the LGM incised valley, meaning that these surfaces formed between 30.0 ka and the time of lowest sea-level during the LGM (20.5 ka; Fig. 3). The Kanto Loam is more common at the edges or in the hollows of the buried terrace than on the buried terrace platform (Fig. 7). This suggests that the top platform of the buried terrace was slightly eroded by waves during the last deglacial sea-level rise.

4.3 Presence and thickness of gravel beds

The distribution of gravel beds at the bases of post-LGM incised-valley fills is illustrated in Fig. 9. Gravel beds are widely present in the Tama River Lowland, and locally in the Tsurumi, Owoka, and Katabira river lowlands and the Tokyo Lowland. Gravel beds are widespread in the Tama River Lowland because of the presence of the T2 and the BG. The gravels forming the T2 and the BG were discharged from the Tama River. Today, 70% of the gravel in the Tama River bed is the product of sandstone beds of the accretionary prism in the Kanto Mountains (Fig. 1c; Nakayama 1954). In contrast, the gravel beds of the buried terrace and the BG are absent from the Tsurumi, Owoka, and Katabira river lowlands, where the post-LGM incised-valley fills directly overlie the Kazusa Group. The gravel beds are absent because the river catchments of the Tsurumi, Owoka, and Katabira Rivers consist of hills and uplands formed of sand and mud of the Kazusa and Shimosa groups, and there is no source of coarse-grained materials originating from hard rock (Fig. 1c). In the Tokyo Lowland, the gravel bed is absent on the T1, but is locally present on the

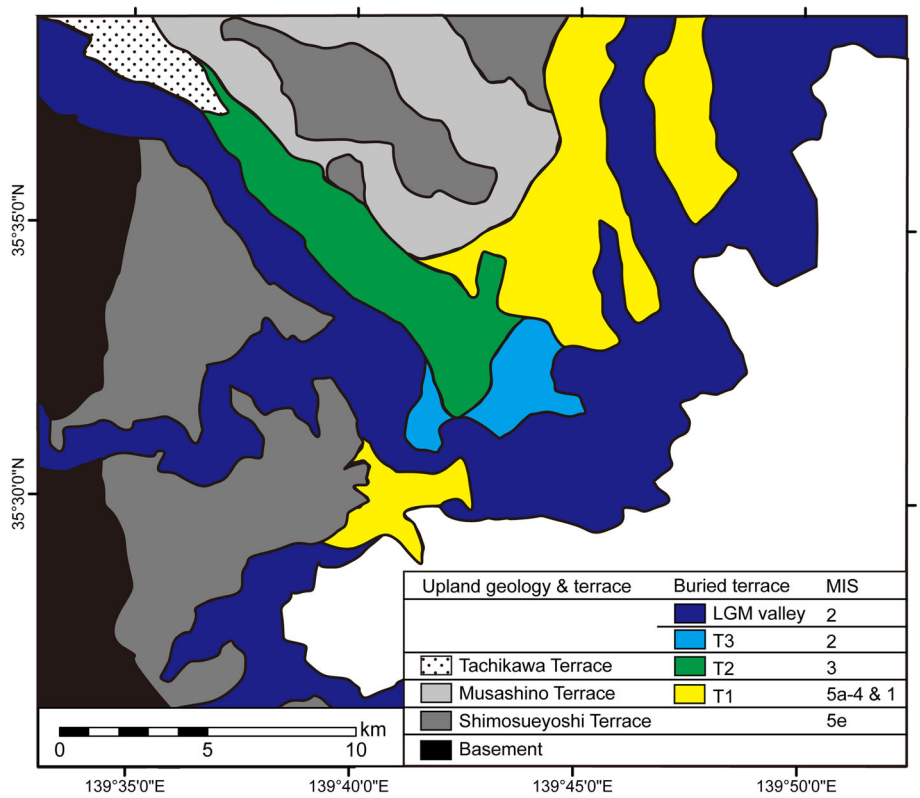

Fig. 8 Classification of upland and buried terraces and LGM incised valleys, all correlated with marine isotope stages. *T1* buried terrace 1, *T2* buried terrace 2, *T3* buried terrace 3, *LGM* valley LGM incised valley. *MIS* marine isotope stage. The T1 partly contains abrasion platforms formed during the middle Holocene sea-level highstand; therefore, it is correlated to MIS 5a–4 and MIS 1

slope and at the base of the Kanda River Valley (Fig. 9). This is because the rivers that formed the T1 did not deposit coarse-grained materials, and the gravel beds on the slope and at the base of the Kanda River Valley are outcrops of the Shimosa Group (Fig. 6, section FF'). The Musashino Upland is within the catchment of the modern Kanda River; however, the modern Kanda River does not have sufficient power to erode and transport the gravels forming the Musashino Terrace. The gravels at the base of the Paleo-Tokyo River Valley were discharged from the Tone River.

The thickness variations of the gravel beds at the bases of the post-LGM incised-valley fills are illustrated in Fig. 10. The thickness of the gravel bed was divided into four categories (0–2, 2–5, 5–10, and 10–22 m) on the basis of the depth of the modern Tama River channel (ca. 5 m; Fig. 4); 2 m and 10 m are approximately half and double the depth of the modern channel, respectively. The gravel bed of the T2 is 2–5 m thick and the BG at the base of the Tama River Valley is 10–22 m thick. This difference arose because the Tama River Valley is narrower (0.8–0.9 km) than the T2 (width 1.9–3.1 km), thus with less accommodation available for alluvial sediments. The BG is thin (5–10 m) in the lower reaches of the Tama River Valley because the valley widens there. BGs in the Tsurumi, Owoka, and Katabira river valleys are locally present and are only several decimeters thick. Lithological description of the borehole logs indicates that the gravel clasts in these BGs are mudstone from the Kazusa Group. The gravel beds on the slope and at the base of the Kanda River Valley are 5–10 m thick, similar to those of the Shimosa Group (Fig. 6, section FF').

5 Discussion

5.1 Formation of buried terraces and incised valleys

Little is known about sea-level changes during the LGM because few sea-level index points are available for this period. Until now, the sea-level fall to the lowest sea-level during the LGM has been considered to be gentle (Siddall et al. 2003; Lambeck et al. 2014) or step-wise (Yokoyama et al. 2018; Ishiwa et al. 2019; Fig. 11). In this study, the existence of the T2 at − 20 m TP, the T3 at − 40 m TP, and the base of the incised valley at − 50 m TP is documented (Fig. 6, section BB'). Based on the presence of the AT tephra on the surfaces and the assumption that the incised valley was formed at the period of lowest sea-level during the LGM, the ages of the T2, T3,

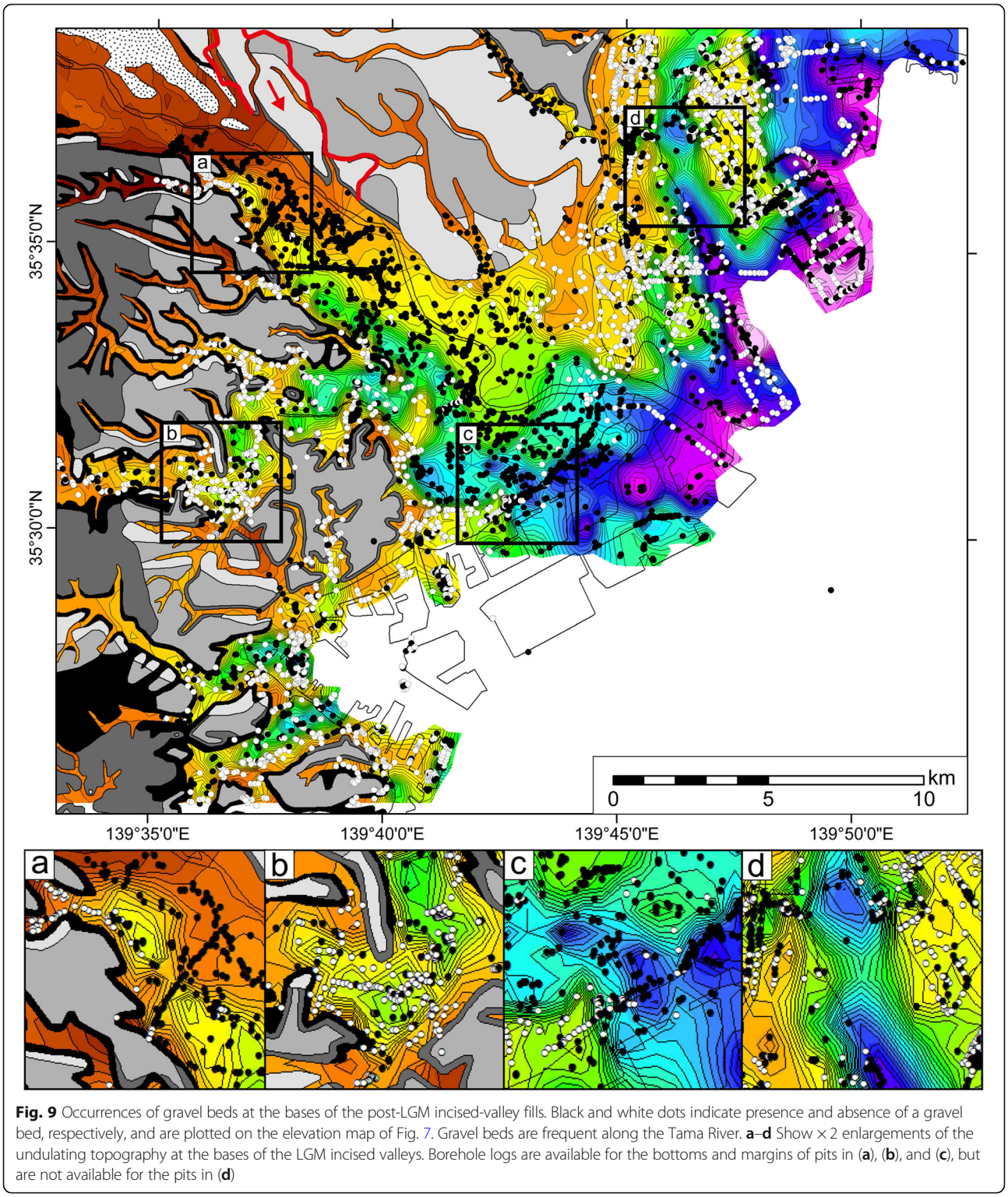

Fig. 9 Occurrences of gravel beds at the bases of the post-LGM incised-valley fills. Black and white dots indicate presence and absence of a gravel bed, respectively, and are plotted on the elevation map of Fig. 7. Gravel beds are frequent along the Tama River. **a**–**d** Show × 2 enlargements of the undulating topography at the bases of the LGM incised valleys. Borehole logs are available for the bottoms and margins of pits in (**a**), (**b**), and (**c**), but are not available for the pits in (**d**)

and incised valleys can be estimated to be > 30.0, 30.0–20.5, and ca. 20.5 ka, respectively. A step-wise fluvial terrace that responds sensitively to sea-level changes will form in a tectonically stable area (Kaizuka 1977). The uplift rate in the Tama River Lowland has been very low since MIS 5e (0.04 m/kyr; Koike and Machida 2001; Okuno et al. 2014). Therefore, the step-wise fluvial terraces consisting of the buried terraces and the incised valley in the Tama River Lowland might reflect two steps of sea-level lowering prior to the lowest sea-level

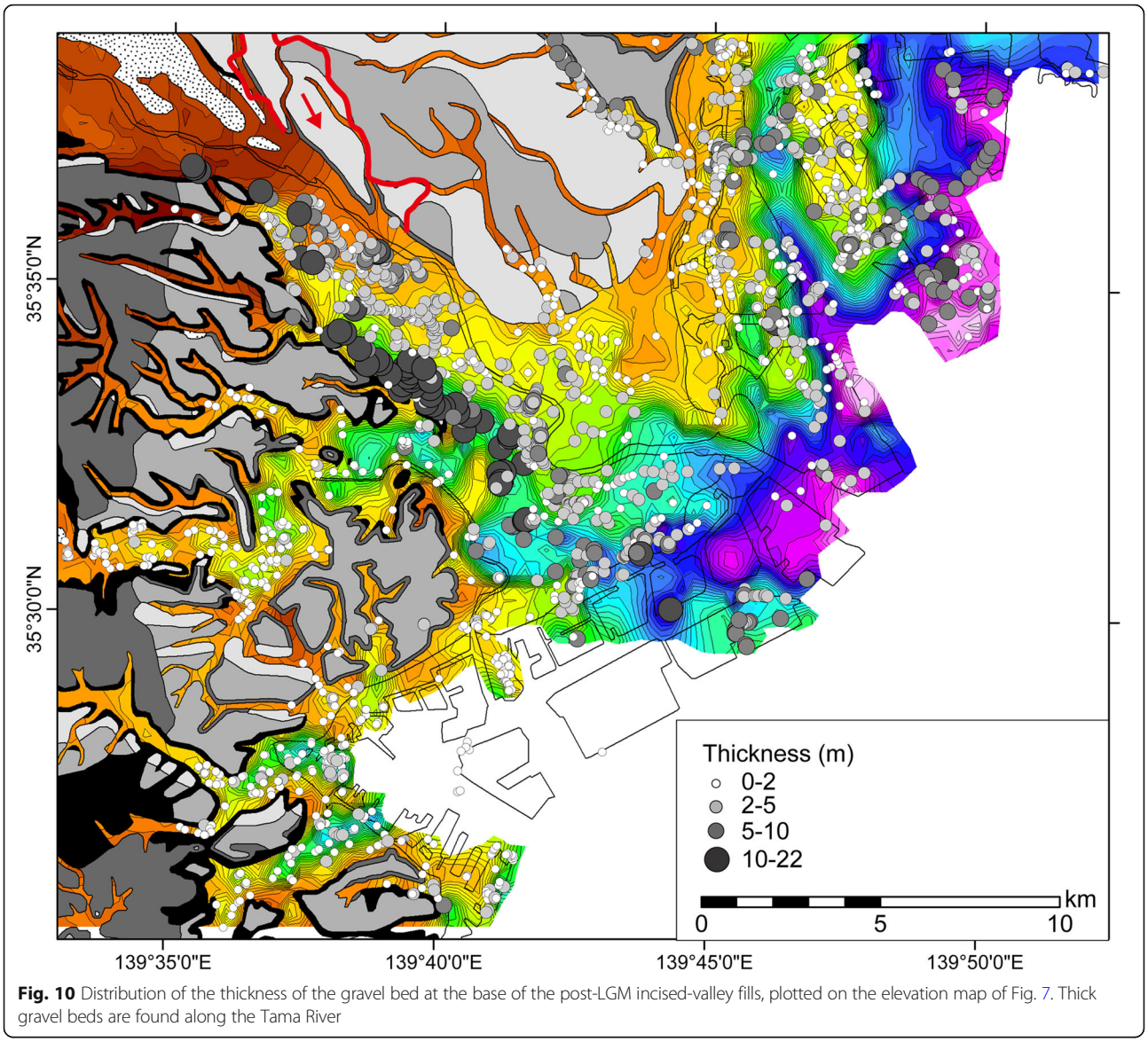

Fig. 10 Distribution of the thickness of the gravel bed at the base of the post-LGM incised-valley fills, plotted on the elevation map of Fig. 7. Thick gravel beds are found along the Tama River

during the LGM. Lambeck et al. (2014) inferred a sea-level plateau before 31 ka, and the T2 formed during formation of this plateau (Fig. 11). Based on Yokoyama et al. (2018), the second sea-level plateau is dated to 29–21.5 ka; the T3 formed during this plateau. The T3 is locally present in the Tama River Valley (Fig. 8); therefore, its continuation in the lower reaches must be confirmed in the future. The formation of the incised valley is estimated to have occurred at the lowest sea-level during the LGM at 21.5–20.5 ka (Yokoyama et al. 2018). The basal age of the BG is regarded as < 30 ka because the LGM incised valleys comprising the BG at the bases dissect the T2. The AT tephra does not overlie the BG anywhere in the Tama River Valley (Fig. 7). In other riverine coastal plains, the LGM incised valleys and T3 might be difficult to discriminate because the distribution of the T3 is presumably local; therefore, the basal age of the BG there can be also regarded as roughly younger than 30 ka.

5.2 Interpretation of undulating topography and basal gravel bed

The thalwegs of the Tama and Tsurumi river valleys calculated from the base of the post-LGM incised-valley fills indicate that the base of the valleys undulate along stream with a series of concave- and convex-upward topography (Fig. 12). The concave-upward topography (scours) are spaced at 1–2-km intervals, and are 1–2 km long, < 1 km wide, and 5–10 m deep. In the Tama and Tsurumi river valleys, multiple borehole logs are available from both the bottoms and the margins of scours, suggesting that the undulating topography is not a result

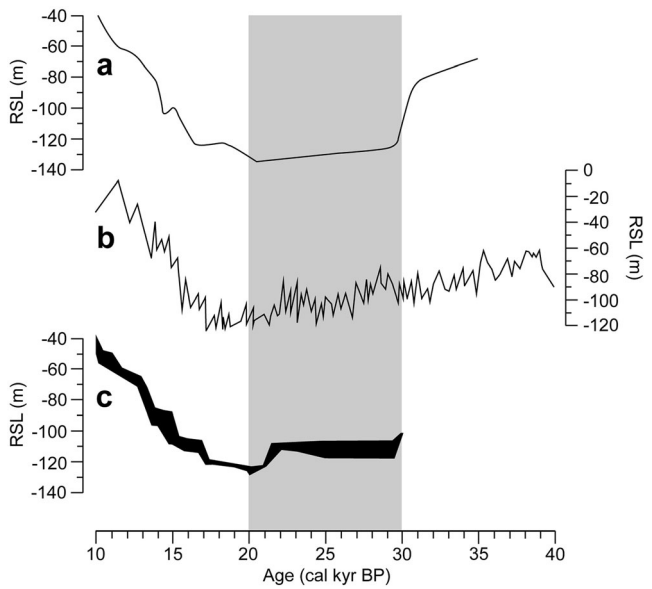

Fig. 11 Sea-level change during the period of formation of the BG. Sea-level curves (**a**), (**b**), and (**c**) are after Lambeck et al. (2014), Siddall et al. (2003), and Yokoyama et al. (2018), respectively. The gray shaded area marks the period of formation of the BG. *RSL* relative sea-level

of abnormal values calculated by mathematical interpolation (Fig. 9a, b, c). However, the undulating topography in the Kanda River Valley, for example, might result from abnormal values calculated by mathematical interpolation because the distribution of borehole logs there is sparse (Figs. 7, 9d).

The undulating topography in the Tama and Tsurumi river valleys is comparable with pools and riffles of braided rivers, which are commonly observed in both flume experiments and modern analogues (Shepherd and Schumm 1974; Keller and Melhorn 1978; Thompson 2018), with pools located at bends and riffles located in straighter river tracts between bends. Pools are deep with low velocities of current during baseflow, while riffles are shallow with high velocities during high flow (Thompson 2018). However, the undulating topography in the Tama and Tsurumi river valleys are large (valley scale) compared to those of simple pools and riffles (channel scale). Furthermore, the gradients of the Tama and Tsurumi river valleys are steeper (3/1000) than those of rivers forming pools and riffles (2/1000; Thompson 2018). Additionally, undulating topography formed by pools and riffles is visible on the tops of gravel beds rather than at their bases (Thompson 2018).

Best and Ashworth (1997) reported scours, 2 km long, 400 m wide, and > 30 m deep in the channel confluences of the Jamuna and Ganges rivers in Bangladesh. These rivers have a combined annual mean discharge of 40,000 m^3/s and a sediment transport rate of 38,000 kg/s per year (Milliman and Farnsworth 2011). The scours are formed during monsoon flood period. Scours at channel confluences have different magnitude due to the scale of gravel bed braided rivers (Best 1988). In a braided river, abundant confluences are formed (e.g., Lane et al. 2003), and scours may have been formed at these confluences. There are a few studies demonstrating basal topography of the gravel beds of the modern braided rivers. Therefore, future study is required; however, the undulating topography in the Tama and Tsurumi river valleys can be tentatively attributed to scours at channel confluences in ancient times, rather than pools and riffles.

The undulating topography, which was formed during the LGM, is more pronounced in the Tsurumi River Valley than in the Tama River Valley (Fig. 12); furthermore, the river incision is deeper in the Tsurumi River Valley than in the Tama River Valley in areas more than 20 km upstream of the Tama River mouth. River erosion, including incision, is controlled by, among other factors, bedrock geology and variations in water and sediment discharges (Whipple et al. 2013). In the Tama and Tsurumi river valleys, the bedrock geology consists of the consolidated Kazusa and Shimosa groups (*N* value > 50), but the distribution of the BG differs in the two valleys. The high sediment discharge and the cover effect of gravel beds on the channel floor (the armoring) resulted in less-pronounced undulating topography and shallower river incision in the Tama River Valley. The cover effect of coarse materials has been commonly detected in abrasion mill experiments (Sklar and Dietrich 2001), modeling (Sklar and Dietrich 2004), flume experiments (Johnson and Whipple 2010), and field observations (Johnson et al. 2009). The cover effect of gravels might also have influenced the sinuosity of the channel forming the valley: the Tama River Valley is less sinuous

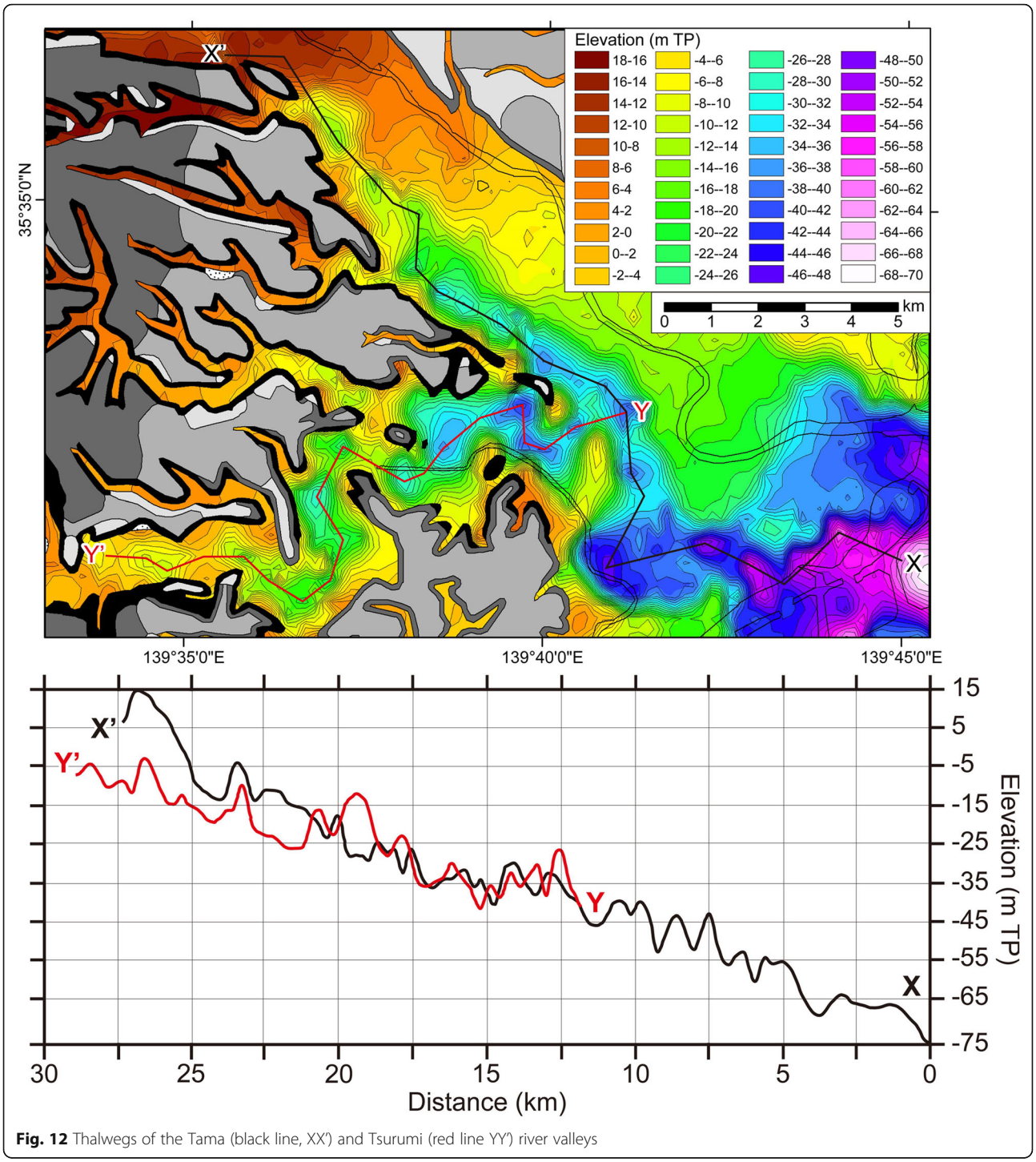

Fig. 12 Thalwegs of the Tama (black line, XX') and Tsurumi (red line YY') river valleys

than the Tsurumi River Valley, likely because erosion in the undercut slope in the Tama River Valley was small due to the cover effect of the abundant gravels. The applicability of the cover effect to both horizontal and vertical river erosion has been confirmed in flume experiments (Shepherd 1972) and theoretically (Turowski 2018).

The gradient of the BG is 3/1000 (Fig. 12), which is three to six times larger than that of the meandering-river segment of the modern Tama River (Kadomura 1961); therefore, river bed erosion coeval with gravel deposition might be enhanced during the sea-level lowering in the LGM with consequent increasing topographic gradient rather than the present day sea-level highstand

(Suzuki 2012, 2013, 2015). The BG majorly consists of gravels larger than 6 cm in diameter (Fig. S1; Tanabe and Nakashima 2016), and the grain size is almost same to that in the modern braided-river segment in the Tama River (Kanto Regional Development Bureau, Ministry of Land, Infrastructure, Transport and Tourism 2017a). These gravels were transported and deposited by bedload during floods (Suzuki 2012, 2013, 2015). The grain size and river gradient of the LGM and present braided rivers are almost same (Figs. 4 and 12). However, the LGM climate is considered to have been cool and dry, and the flood intensity and the sediment discharge by rivers have been regarded as low compared with those of today (Chabangborn et al. 2014); therefore, the grain size of the gravels of the BG should be smaller than that in the present braided-river segment. To explain the relatively large volume of the BG deposited during the LGM (Fig. 10), recycle of gravels from the post-MIS 5a fluvial terraces must be considered (Fig. 1c). Comparably large gravels of the BG instead of less intensity of floods during the LGM can be also explained by this recycle.

6 Conclusions

In this study, we revealed the detailed topography of the LGM incised valley of the Tama River Lowland, central Japan, by analyses of 4702 borehole logs. The spatial distribution of the incised valley was reconstructed by mathematically interpolating (Kriging) the depth of the base of the incised valley identified in each borehole log. From this analysis, undulating topography at the base of the incised valley was confirmed. This undulating topography, which consists of a series of pits 1–2 km long, < 1 km wide, and 5–10 m deep that occur at 1–2-km intervals, can be identifiable as scouring at braided-river channel confluences. At least one borehole log is available for each 187 m × 187 m grid cell and multiple borehole logs are available from both bottom and margin portions of the scouring; therefore, this topography is not a representation of abnormal values calculated by Kriging.

In the Tama River Valley, the T2 at − 20 m TP, which is overlain by the AT tephra, is dissected by the T3 at − 40 m TP and the LGM incised valley at − 50 m TP, neither of which are overlain by the AT tephra. The Tama River Lowland has been tectonically stable since MIS 5e. Therefore, these fluvial terraces might have formed as a result of step-wise sea-level lowering before the lowest sea-level during the LGM. The T2, the T3, and the LGM incised valley might have formed during sea-level plateaus at > 30.0, 30.0–21.5, and 21.5–20.5 ka, respectively. The last plateau corresponds to the lowest sea-level during the LGM. This is a first finding, which support the LGM sea-level plateau at 30.0–21.5 ka in Japan.

The Tama River Valley (depth − 70 m TP) and the Tsurumi River Valley (depth − 40 m TP) lie beneath the Tama River Lowland. These valleys merge 10 km upstream of the modern Tama River mouth. The bedrock of both valleys is the consolidated Kazusa and Shimosa groups; however, the undulating topography is more pronounced and the river incision depth and sinuosity are greater in the Tsurumi River Valley than in the Tama River Valley. The major differences between the two valleys arose from differences in sediment discharge and the presence of the BG, which in turn led to a difference in the cover effect. The undulating topography is pronounced and the river incision depth and sinuosity are larger in the Tsurumi River Valley because it lacked the cover effect of the BG. Clear evidence of the cover effect on the LGM incised valleys has been never demonstrated before.

In this study, we have confirmed that the basal age of the BG is < 30 ka because the LGM incised valleys comprising the BG at the bases dissect the T2. In other riverine coastal plains, the LGM incised valleys and T3 might be difficult to discriminate because the distribution of the T3 is presumably local; therefore, the basal age of the BG can be also regarded as roughly younger than 30 ka there. However, furthermore age data is required, and geomorphological and depositional settings must be considered for the adaptation of this age to the BGs in other riverine coastal plains.

7 Supplementary Information

The online version contains supplementary material available at https://doi.org/10.1186/s40645-021-00411-0.

Additional file 1: Fig. S1. Sedimentary logs of five stratotype cores obtained by the Geological Survey of Japan (Tanabe and Nakashima, 2016). **Table S1.** Sampling locations of stratotype cores used in this study. **Table S2.** Radiocarbon dates from the stratotype cores. Measured ^{14}C ages of GaK were converted into conventional ^{14}C age by assuming delta ^{13}C values of shells and peats as 0 and -27.5‰, respectively.

Acknowledgements

We thank the Civil Engineering Support and Training Center, Bureau of Construction, Tokyo Metropolitan Government; the Bureau of Port and Harbour, Tokyo Metropolitan Government; and the Bureau of Environment, Kawasaki City, for providing the XML data of borehole logs. We thank valuable comments from Yoshiki Saito, Marco Mancini, and two anonymous reviewers, which greatly improved the manuscript.

Availability of data and material

Please contact author for data requests.

Authors' contributions

ST designed and performed this study and wrote the manuscript. YI created the voxel model. Both authors read and approved the final manuscript.

Funding

This work was financially supported by the National Institute of Advanced Industrial Science and Technology (AIST) research program "Geological and active faults survey project in coastal areas of Japan".

Competing interests
The authors declare that they have no competing interest.

Author details
[1]Geological Survey of Japan, AIST, Central 7, Higashi 1-1-1, Tsukuba 305-8567, Japan. [2]Fukuoka University, Nanakuma 8-19-1, Jonan-ku, Fukuoka 814-0180, Japan.

Received: 7 October 2020 Accepted: 27 January 2021
Published online: 04 March 2021

References

Anderson JB, Rodriguez AB (eds) (2008) Response of Upper Gulf Coast Estuaries to Holocene climate change and sea-level rise. GSA Spec Pap 443
Best JL (1988) Sediment transport and bed morphology at river channel confluences. Sedimentology 35:481–498
Best JL, Ashworth PJ (1997) Scour in large braided rivers and the recognition of sequence stratigraphic boundaries. Nature 387:275–277
Boyd R, Dalrymple R, Zaitlin BA (1992) Classification of clastic coastal depositional environments. Sediment Geol 80:139–150
Bureau of Port and Harbour, Tokyo Metropolitan Government (2001) Underground Geological Map of the Tokyo Bay, 2nd edn. (in Japanese)
Catuneanu O (2006) Principles of Sequence Stratigraphy. Elsevier, Amsterdam
Chabangborn A, Brandefelt J, Wohlfarth B (2014) Asian monsoon climate during the Last Glacial Maximum: paleo-data-model comparisons. Boreas 43:220–242
Chaumillon E, Proust JN, Menier D, Weber N (2008) Incised-valley morphologies and sedimentary-fills within the inner shelf of the Bay of Biscay (France): A synthesis. J Marine Systems 72:383–396
Chaumillon E, Weber N (2006) Spatial variability of modern incised valleys on the French Atlantic Coast: Comparison between the Charente and the Lay-Sèvre incised valleys. SEPM Spec Publ 85:57–85
Civil Engineering Support and Training Center, Bureau of Construction, Tokyo Metropolitan Government (2019) Underground geology of Tokyo, GIS Ver. http://www.kensetsu.metro.tokyo.jp/jigyo/tech/start/03-jyouhou/geo-web/00-index.html.
Dalrymple RW, Boyd R, Zaitlin BA (eds) (1994) Incised-valley systems: origin and sedimentary sequences. SEPM Spec Publ 51
Dalrymple RW, Leckie DA, Tillman RW (eds) (2006) Incised Valleys in Time and Space. SEPM Spec Publ 85
Davis RA Jr, Hayes MO (1984) What is a wave-dominated coast? Mar Geol 60: 313–329
Editorial Committee of "Story of N-value" (1998) Story of N-value. Riko Tosho, Tokyo (in Japanese)
Endo T, Kawashima S, Kawai M (2001) Historical review of development of land subsidence and its cease in Shitamachi Lowland, Tokyo. J Japan Soc Eng Geol 42:74–87 (in Japanese with English abstract)
Geological Survey of Japan, AIST (ed) (2019) Seamless digital geological map of Japan V2, 1: 200,000. https://gbank.gsj.jp/seamless/.
Grant KM, Rohling EJ, Bar-Matthews M, Ayalon A, Medina-Elizalde M, Bronk Ramsey C, Satow C, Roberts AP (2012) Rapid coupling between ice volume and polar temperature over the past 150,000 years. Nature 491:744–747
Hasada K, Hori K (2016) Carbon storage in a Holocene deltaic sequence: an example from the Nobi Plain, central Japan. Quatern Int 397:194–207
Horner SC, Hubbard SM, Martin HK, Hagstorm CA, Leckie DA (2019) The impact of Aptian glacio-eustacy on the stratigraphic architecture of the Athabasca Oil Sands, Alberta, Canada. Sedimentology 66:1600–1642
Ielpi A, Ghinassi M (2014) Genetically related incised valleys and deltas: sequence and modern analogue modelling from the nonmarine Santa Barbara coalfield, Late Pliocene, Italy. J Sediment Res 84:645–663
Ishihara T, Sugai T (2017) Eustatic and regional tectonic controls on late Pleistocene paleovalley morphology in the central Kanto Plain, Japan. Quatern Int 456:69–84
Ishihara T, Sugai T, Hachinohe S (2012) Fluvial response to sea-level changes since the latest Pleistocene in the near-coastal lowland, central Kanto Plain, Japan. Geomorphology 147–148:49–60
Ishihara Y, Miyazaki Y, Eto C, Fukuoka S, Kimura K (2013) Shallow subsurface three-dimensional geological model using borehole logs in Tokyo Bay area, central Japan. J Geol Soc Japan 119:554–566 (in Japanese with English abstract)
Ishiwa T, Yokoyama Y, Okuno J, Obrochta S, Uehara K, Ikehara M, Miyairi Y (2019) A sea-level plateau preceding the Marine Isotope Stage 2 minima revealed by Australian sediments. Sci Rep 9: 6449. doi.org/10.1038/s41598-019-42573-4
Ito Y, Oguchi T, Masuda F (2018) Late Quaternary depositional sequence and landforms in relation to sea-level changes in the Osaka intra-arc basin, Japan: a borehole database analysis. Quatern Int 471:298–317
Johnson JPL, Whipple KX (2010) Evaluating the controls of shear stress, sediment supply, alluvial cover, and channel morphology on experimental bedrock incision rate. J Geophys Res 115:F02018. https://doi.org/10.1029/2009JF001335
Johnson JPL, Whipple KX, Sklar LS, Hanks TC (2009) Transport slopes, sediment cover, and bedrock channel incision in the Henry Mountains, Utah. J Geophys Res 114:F02014. https://doi.org/10.1029/2007JF000862
Kadomura H (1961) Geomorphology of the Tama River Lowland. Geogr Sci 1:16–26 (in Japanese)
Kaizuka S (1977) Geomorphology of Japan: characteristics and formation. Iwanami Shoten, Tokyo (in Japanese)
Kaizuka S, Matsuda I (eds) (1982) Active tectonics and geomorphic division of the Tokyo Metropolitan area and damage ratio due to the Kanto Earthquake of 1923. 1:200,000. Naigai Chizu, Tokyo (in Japanese)
Kaizuka S, Naruse Y, Matsuda I (1977) Recent formations and their topography in and around Tokyo Bay, central Japan. Quatern Res 8:32–50
Kanto Regional Development Bureau, Ministry of Land, Infrastructure, Transport and Tourism (2017a) Maintenance plan of the Tama River system. http://www.ktr.mlit.go.jp/ktr_content/content/000669893.pdf.
Kanto Regional Development Bureau, Ministry of Land, Infrastructure, Transport and Tourism (2017b) Maintenance plan of the Tsurumi River system. http://www.ktr.mlit.go.jp/ktr_content/content/000669618.pdf.
Kawasaki City (2019) Guide map of Kawasaki City, geological map collection. http://kawasaki.geocloud.jp/webgis/?mp=38.
Keller EA, Melhorn WN (1978) Rhythmic spacing and origin of pools and riffles. GSA Bull 89:723–730
Koike K, Machida H (eds) (2001) Atlas of Quaternary marine terraces in the Japanese islands. University of Tokyo Press, Tokyo (in Japanese)
Lambeck K, Rouby H, Purcell A, Sun Y, Sambridge M (2014) Sea level and global ice volumes from the Last Glacial Maximum to the Holocene. Proc Natl Acad Sci 111:15296–15303
Lane SN, Westaway RM, Hicks DM (2003) Estimation of erosion and deposition volumes in a large, gravel-bed, braided river using synoptic remote sensing. Earth Surf Process Landf 28:249–271
Machida H, Arai F (2003) Atlas of Tephra in and around Japan. University of Tokyo Press, Tokyo (in Japanese)
Matsuda I (1973) Recent deposits and buried landforms in the Tamagawa Lowland. Geogr Rev Japan 46:339–356 (in Japanese with English abstract)
Matsuda I (1974) Distribution of the recent deposits and buried landforms in the Kanto Lowland, central Japan. Geogr Rep Tokyo Metropolitan Univ 9:1–36
Matsushima Y (1973) Preliminary report on the molluscan assemblages from the alluvial deposits in Yokohama City. Bull Kanagawa Pref Mus 6:7–19 (in Japanese with English abstract)
Matsushima Y (ed) (1987) The geological studies on the Alluvium deposits in the Tama and Tsurumi Rivers Lowland, Kawasaki. Committee of document collection for the Kawasaki Museum (in Japanese)
Matsushima Y, Yamaguchi Y (1987) Radiocarbon ages of the molluscan fossils and peat from the Alluvium deposits in Yokohama City. Nat Hist Rep Kanagawa 8: 37–40 (in Japanese)
Miall AD (1992) Alluvial deposits. In: Walker RG, James NP (eds) Facies models: response to sea level change. Geol Assoc Canada, pp 119–142
Milli S, Mancini M, Moscatelli M, Stigliano F, Marini M, Cavinato GP (2016) From river to shelf, anatomy of a high-frequency depositional sequence: The Late Pleistocene to Holocene Tiber depositional sequence. Sedimentology 63: 1886–1928
Milliman JD, Farnsworth KL (2011) River discharge to the coastal ocean: a global synthesis. Cambridge Univ Press
Ministry of Land, Infrastructure, Transport and Tourism (2016) A guidebook for submission of electric formatted report on geology and soil investigation. http://www.cals-ed.go.jp/mg/wp-content/uploads/boring71.pdf.
Mitamura M, Hashimoto M (2004) Spatial distribution with the drilling database on the Basal Gravel Bed of the Namba Formation in the Osaka Plain, southwest Japan. The Quaternary Research 43:253–264 (in Japanese with English abstract)
Nakayama M (1954) Roundness of pebbles of the Tama River, Kanto district. Geogr Rev Japan 27:497–506 (in Japanese with English abstract)

Nakazawa T, Cho I, Sakata K, Nakazato H, Hongo M, Naya T, Nonogaki S, Nakayama T (2019) Stratigraphy, distribution patterns, and ground motion characteristics of the Pleistocene Setagaya and Tokyo formations beneath the Musashino Upland, Setagaya, Tokyo, central Japan. J Geol Soc Japan 125: 367–385 (in Japanese with English abstract)
Oka S, Kikuchi T, Katsurajima S (1984) Geology of the Tokyo-Seinambu District. Quadrangle Series, 1:50,000. Geol Surv Japan (in Japanese with English abstract)
Okuma T (1981) Influences of the river modification and the eruption of the Asama volcano at the beginning of the early modern period. Urban Kubota 19:18–31 (in Japanese)
Okuno J, Nakada M, Ishii M, Miura H (2014) Vertical tectonic crustal movements along the Japanese coastlines inferred from late Quaternary and recent relative sea-level changes. Quatern Sci Rev 91:42–61
Pollution Research Institute, Yokohama City (1988) Report on soft ground in Yokohama City. Documents of Pollution Research Institute, Yokohama City 83 (in Japanese)
Port of Tokyo Geological Research Group (2000) Stratigraphy of the Port of Tokyo, Japan. Monogr Assoc Geol Collab Japan 47:10–22 (in Japanese with English abstract)
Public Works Research Institute (2019) Kunijiban. http://www.kunijiban.pwri.go.jp/jp/.
Reimer PJ, Bard E, Bayliss A, Beck JW, Blackwell PG, Bronk Ramsey C, Buck CE, Cheng H, Edwards RL, Friedrich M, Grootes PM, Guilderson TP, Haflidason H, Hajdas I, Hatté C, Heaton TJ, Hoffmann DL, Hogg AG, Hughen KA, Kaiser KF, Kromer B, Manning SW, Niu M, Reimer RW, Richards DA, Scott EM, Southon JR, Staff RA, Turney CSM, van der Plicht J (2013) IntCal13 and Marine13 radiocarbon age calibration curves 0–50,000 years cal BP. Radiocarbon 55: 1869–1887
Shepherd RG (1972) Incised river meanders: Evolution in simulated bedrock. Science 178:409–411
Shepherd RG, Schumm SA (1974) Experimental study of river incision. GSA Bull 85:257–268
Siddall M, Rohling EJ, Almogi-Labin A, Hemleben C, Meischner D, Schmelzer I, Smeed DA (2003) Sea-level fluctuations during the last glacial cycle. Nature 423:853–858
Sklar LS, Dietrich WE (2001) Sediment and rock strength controls on river incision into bedrock. Geology 29:1087–1090
Sklar LS, Dietrich WE (2004) A mechanistic model for river incision into bedrock by saltating bed load. Water Resour Res 40:W06301. https://doi.org/10.1029/2003WR002496
Smith VC, Staff RA, Blockley SPE, Bronk Rmasey C, Nakagawa T, Mark DF, Takemura K, Danhara T, Suigetsu 2006 project members (2013) Identification and correlation of visible tephras in the Lake Suigetsu SG06 sedimentary archive, Japan: chronostratigraphic markers for synchronising of east Asian/west Pacific palaeoclimatic records across the last 150 ka. Quatern Sci Rev 67: 121–137
Stuiver M, Braziunas TF (1993) Modelling atmospheric ^{14}C influences and ^{14}C ages of marine samples back to 10,000 BC. Radiocarbon 35:137–189
Stuiver M, Reimer PJ, Reimer RW (2019) CALIB:7.1 http://calib.org/calib/.
Sugimoto M, Umehara J (1994) Study on ground subsidence of soft layers (part 7): Measurement of settlement in the lowland of Ohuoka and Katabira rivers, Yokohama City. Annu Rep Yokohama Env Res Inst 18:105–110 (in Japanese)
Suzuki K (2012) Gravel size distribution of Kizu River in the southern part of Kyoto Prefecture, Japan. The research journal of the Department of Teacher Education, Kinki University 24:1–16
Suzuki K (2013) Grain size distribution of the gravel deposits in the Yodo River system, Japan. The research journal of the Department of Teacher Education, Kinki University 24:17–38
Suzuki K (2015) Relationship between the river-bed gradient and gravel size distribution in the Yamato River, Japan. J Sedimentological Soc Japan 74: 113–122
Tanabe S (2020) Stepwise accelerations in the rate of sea-level rise in the area north of Tokyo Bay during the Early Holocene: Quatern Sci Rev 248, 106575
Tanabe S, Ishihara T, Komatsubara T (2014) Undulating topography at the base of the alluvium: preliminary interpretation on the formation. Bull Geol Surv Japan 65:45–55 (in Japanese with English abstract)
Tanabe S, Ishihara Y (2015) Spatial distribution of lithology and *N*-value in the Tama River Lowland, central Japan. GSJ Int Rep 68:73–81 (in Japanese with English abstract)
Tanabe S, Ishihara Y (2020) Incised-valley topography formed into the Last Glacial Maximum beneath the southern area of the Tokyo Lowland, central Japan. Bull Geol Surv Japan 71:201–213 (in Japanese with English abstract)
Tanabe S, Ishihara Y, Nakanishi T (2010) Stratigraphy and physical property of the Alluvium under the Tokyo and Nakagawa Lowlands, Kanto Plain, central Japan: implications for the Alluvium subdivision. J Geol Soc Japan 116:85–98 (in Japanese with English abstract)
Tanabe S, Nakanishi T, Ishihara Y, Nakashima R (2015) Millennial-scale stratigraphy of a tide-dominated incised valley during the last 14 kyr: Spatial and quantitative reconstruction in the Tokyo Lowland, central Japan. Sedimentology 62:1837–1872
Tanabe S, Nakanishi T, Kimura K, Hachinohe S, Nakayama T (2008) Basal topography of the Alluvium under the northern area of the Tokyo Lowland and Nakagawa Lowland, central Japan. Bull Geol Surv Japan 59:497–508 (in Japanese with English abstract)
Tanabe S, Nakashima R (2016) Lithofacies, biofacies and radiocarbon dates of the Alluvium in core sediments obtained from the Tamagawa Lowland, Japan. GSJ Int Rep 71:109–120 (in Japanese with English abstract)
Thompson DM (2018) Pool-riffle sequences. Reference Module in Earth Systems and Environmental Sciences. doi.org/https://doi.org/10.1016/B978-0-12-409548-9.11029-2
Turowski JM (2018) Alluvial cover controlling the width, slope and sinuosity of bedrock channels. Earth Surf Dynam 6:29–48
van Wagoner JC, Posamentier HW, Mitchum RM, Vail PR, Sarg JF, Louit TS, Hardenbol J (1988) An overview of the fundamentals of sequence stratigraphy and key definitions. SEPM Spec Publ 42:39–45
Walsh JP, Wiberg P, Aalto R (eds) (2016) Source-to-sink systems: sediment & solute transfer on the Earth Surface. Earth Sci Rev 153
Whipple KX, DiBiase RA, Crosby BT (2013) Bedrock rivers. In: Wohl E (ed) Treatise on Geomorphology, Fluvial Geomorphology, vol 9. Academic Press, California, pp 550–573
Yamaguchi M, Sugai T, Ogami T, Fujiwara O, Ohmori H (2006) Three-dimensional structures of the latest Pleistocene to Holocene sequence at Nobi Plain, central Japan. J Tokyo Geogr Soc 115:41–50 (in Japanese with English abstract)
Yokohama City (2019) Jiban View. http://wwwm.city.yokohama.lg.jp/index.asp?dtp=3&adl=%2C3.
Yokoyama Y, Esat TM, Thompson WG, Thomas AL, Webster JM, Miyairi Y, Sawada C, Aze T, Matsuzaki H, Okuno J, Fallon S, Braga J, Humblet M, Iryu Y, Potts DC, Fujita K, Suzuki A, Kan H (2018) Rapid glaciation and a two-step sea level plunge into the Last Glacial Maximum. Nature 559:603–607
Zaitlin BA, Dalrymple RW, Boyd R (1994) The stratigraphic organization of incised-valley systems: origin and sedimentary sequences. SEPM Spec Publ:45–60

Publisher's Note